Uniform approximation in scattering by spheres

1988 J. Phys. A: Math. Gen. 21 81

(http://iopscience.iop.org/0305-4470/21/1/017)

J. Phys. A: Math. Gen. **21** (1988) 81-109. Printed in the UK

Uniform approximation in scattering by spheres

H M Nussenzveig†
NASA Goddard Space Flight Center, Greenbelt, MD 20771, USA

Received 6 March 1987, in final form 29 June 1987

Abstract. A new approximation to the scattering amplitude from an impenetrable sphere at short wavelengths is developed. In contrast with Fock's theory, it remains valid at large scattering angles, where it can be matched with the usual semiclassical approximations. The accuracy, both for the magnitude and for the phase of the scattering amplitude, is improved by one or more orders of magnitude over previously known approximations. The approximation remains accurate even at size parameters below unity, bridging the gap between short and long wavelengths. Large-angle diffraction can be interpreted as a tunnelling effect.

1. Introduction

Uniform semiclassical approximations to the scattering of non-relativistic particles by central potentials having long-range tails that lead to forward diffraction peaks have been developed by Berry (1969). In contrast with transitional approximations, valid only very close to the forward direction and failing to merge smoothly with the ordinary semiclassical (WKB) formulae at larger angles, uniform approximations remain valid near to or far from the forward direction. The results depend on the form of the potential tail, because near-forward scattering is associated with large impact parameters.

Corresponding uniform approximations have not been developed, thus far, for the scattering by cutoff potentials, such as square wells or barriers. Closely related problems exist in the scattering of classical (e.g. acoustic or electromagnetic) waves by spherical particles. In view of the manifold practical applications of these models, as well as of their role as paradigms in scattering theory, this is a serious omission, which we address in the present work.

The physical origin of near-forward scattering from such cutoff potentials is quite different from that found for potentials with tails because of the significant contribution from impact parameters very close to the 'edges' of the spherical scatterer, i.e. from the neighbourhood of grazing incidence.

In a celebrated series of papers (see Fock 1965), Fock developed a theory of diffraction by curved edges. The results are expressed in terms of new diffraction integrals, known as Fock functions. By applying complex angular momentum theory to short-wavelength scattering by homogeneous spheres (Nussenzveig 1965, 1969), it

† Permanent address: Departamento de Física, Pontifícia Universidade Católica, Rio de Janeiro, RJ 22452, Brazil.

0305-4470/88/010081+29$02.50

was shown that the near-forward scattering amplitude can be expressed in terms of generalised Fock functions, within an angular domain

$$0 \leqslant \theta \leqslant \gamma \tag{1.1}$$

where θ is the scattering angle and

$$\gamma \equiv (2/\beta)^{1/3} \qquad \beta \equiv ka \tag{1.2}$$

k being the wavenumber and a the radius of the sphere.

Unfortunately, however, the Fock approximation is a transitional approximation. While it can yield accurate results within the domain (1.1) for $\beta \gg 1$, it fails to bridge the gap between $\theta \sim \gamma$ and $\theta \gg \gamma$. This is the crucial region in which the transition to wide-angle scattering takes place.

In practical applications of Mie scattering, where numerical results are obtained by summation of the exact partial-wave series, a major stumbling block is that the required computer time grows roughly linearly with β. Complex angular-momentum theory (Nussenzveig 1979) provides size-independent asymptotic approximations for $\beta \gg 1$. However, since the angular distribution becomes increasingly peaked around the forward direction as β increases, it is essential to obtain accurate approximations to Fock-type scattering, valid over the broadest possible range of θ and β.

Other angular domains in acoustic and Mie scattering, away from the near-forward region, are of 'Fock type' (Nussenzveig 1969, 1979), providing additional incentive for the development of a uniform approximation. While several approaches to this end have been suggested (Ludwig 1966, 1967, 1969, Lewis *et al* 1967, Borovikov and Kinber 1974), none seems to have led to an explicit expression for the scattering amplitude.

In this paper, to avoid inessential complications, we derive the uniform approximation in connection with the simplest example, scalar scattering by a sphere with a Dirichlet boundary condition (quantum hard sphere or acoustic soft sphere, as in Nussenzveig (1965)). In spite of its simplicity, this problem has interesting applications (hard core in nuclear interactions, hard-sphere gas). It may also be regarded as the simplest model of diffraction by a three-dimensional obstacle, so that a thorough understanding of the solution is of fundamental interest in the theory of wave propagation.

The uniform approximation has already been extended to a variety of other problems in acoustic scattering (rigid sphere) and electromagnetic scattering (perfectly conducting sphere, general Mie scattering). The results, including detailed comparisons with the corresponding exact solutions, will be reported in a forthcoming series of papers (Nussenzveig and Wiscombe 1987).

The basic idea is to take advantage of the freedom associated with complex angular momentum to derive rapidly convergent integral and series representations of the scattering amplitude. In § 2, we recall two basic representations, already derived in Nussenzveig (1965): an 'inner' representation, applicable around $\theta = 0$, and an 'outer' one, applicable up to $\theta = \pi$. Both are exact, and we verify their equivalence by transforming one of them into the other one at intermediate scattering angles. This provides insight into the matching mechanism, which is very helpful for constructing the uniform approximation.

The outer approximation (§ 3) is the sum of the WKB expansion and surface wave contributions, associated with 'creeping waves' generated at grazing incidence. The WKB expansion arises from a real saddle point in the complex angular-momentum plane. It is associated with classical paths, representing reflection from the surface of

the sphere. As $\theta \to 0$, this approaches glancing reflection, and the whole approximation breaks down; the forward direction is a focal line. To improve the accuracy and domain of applicability of the outer approximation, we evaluate WKB corrections up to second order.

In § 4, we derive a uniform asymptotic approximation for one term of the inner representation, the diffraction amplitude, which represents the blocking effect of the scatterer and depends only on its geometrical shape. In the approximation of classical diffraction theory, it corresponds to the well known Airy pattern, associated with the forward diffraction peak.

We consider next the crucial terms arising from near-edge incidence. The contribution from rays travelling above the edge, but still interacting with the scatterer by tunnelling through the centrifugal barrier to the surface, is uniformly approximated in § 5.

The near-edge contribution from rays incident below the edge (§ 6) is the hardest one to evaluate. For large enough θ, it yields the geometrical reflection saddle point, linking up with the WKB contribution. One must follow up the 'birth' of this saddle point, and modify the path of integration when it is fully developed. The most suitable path is a hybrid between a steepest-descent path and a stationary-phase one, each of them yielding half of the WKB contribution in the limit of large θ. The evaluation of this term completes the derivation of the uniform approximation. The corresponding expression for the total cross section is also obtained in § 6.

In § 7, we establish the connection with previously known results, including the Fock approximation. The resulting transitional approximations, though considerably less accurate than the uniform one, may be useful in the limit of small θ and γ.

The physical interpretation of the results is discussed in § 8. We analyse the relationship with general semiclassical dynamics. The Leontovich–Fock physical picture of edge effects, based on the concept of transverse diffusion (Malyuzhinets 1959), is inadequate. In complex angular-momentum theory, edge diffraction appears as a tunnelling effect.

Finally, in § 9, the accuracy and the domain of applicability of the uniform approximation are discussed. A few representative examples of numerical comparisons with the exact solution are given. The uniform approximation is found to be, typically, one to two orders of magnitude more accurate than previously known approximations. In other applications (Nussenzweig and Wiscombe 1987) still higher accuracy is found. In contrast with the Fock approximation, it enables us to make the transition to wide-angle scattering, so that, by combining it with the outer approximation, we can accurately reproduce both the modulus and the phase of the scattering amplitude for all values of θ. Furthermore, it remains reasonably accurate down to $\beta \sim \frac{1}{2}$, so that it also bridges the gap between short- and long-wavelength scattering.

2. Exact representations and matching

The dimensionless total scattering amplitude for scalar plane-wave incidence on a sphere of radius a, with a Dirichlet boundary condition, is given by the partial-wave expansion

$$F(\beta, \theta) \equiv f(k, \theta)/a$$
$$= \frac{\mathrm{i}}{\beta} \sum_{l=0}^{\infty} (l+\tfrac{1}{2})[1 - S_l(\beta)] P_l(\cos\theta) \tag{2.1}$$

where $\beta = ka$ is the size parameter, $P_l(\cos\theta)$ is the Legendre polynomial and

$$S_l(\beta) = -h_l^{(2)}(\beta)/h_l^{(1)}(\beta) \tag{2.2}$$

is the S function for the lth partial wave; $h_l^{(1,2)}(\beta)$ are the spherical Hankel functions.

The normalised differential cross section is

$$(\mathrm{d}\sigma/\mathrm{d}\Omega)/(a^2/4) = 4|F(\beta,\theta)|^2 \tag{2.3}$$

which approaches unity in the classical (geometrical optics) limit. The normalised total cross section, which we refer to as 'extinction efficiency', by analogy with light scattering nomenclature (van de Hulst 1957), is given by the optical theorem as

$$Q_{\mathrm{ext}}(\beta) \equiv \sigma(\beta)/(\pi a^2) = 4\,\mathrm{Im}\,F(\beta,0)/\beta. \tag{2.4}$$

When $\beta \gg 1$, an accurate evaluation of the partial-wave series (2.1) requires summing

$$l_+ \approx \beta + 4\beta^{1/3} \tag{2.5}$$

terms (Wiscombe 1980). The application of complex angular-momentum theory to obtain asymptotic approximations to $F(\beta,\theta)$ is discussed in Nussenzveig (1965).

For $0 < \theta \leqslant \pi$, we may employ the exact representation (Nussenzveig 1965, equations (9.75) and (9.79))

$$F(\beta,\theta) = F_{\mathrm{r}}(\beta,\theta) + F_{\mathrm{s}}(\beta,\theta) \qquad 0 < \theta \leqslant \pi \tag{2.6}$$

where the reflection amplitude $F_{\mathrm{r}}(\beta,\theta)$ is given by

$$\begin{aligned} F_{\mathrm{r}}(\beta,\theta) &= -\frac{\mathrm{i}}{\beta}\int_{\bar{\sigma}\infty}^{-\bar{\sigma}\infty} S(\lambda,\beta)Q_{\lambda-1/2}^{(1)}(\cos\theta)\lambda\,\mathrm{d}\lambda \\ &= \frac{\mathrm{i}}{\beta}\int_{\bar{\sigma}\infty}^{0} S(\lambda,\beta)P_{\lambda-1/2}(-\cos\theta)\tan(\pi\lambda)\exp(-\mathrm{i}\pi\lambda)\lambda\,\mathrm{d}\lambda \end{aligned} \tag{2.7}$$

with

$$S(\lambda,\beta) = -H_\lambda^{(2)}(\beta)/H_\lambda^{(1)}(\beta) \tag{2.8}$$

denoting the extension of the S function (2.2) to complex angular momentum λ (physical values $l+\frac{1}{2}$); $H_\lambda^{(1,2)}$ are Hankel's functions of the first and second kind, respectively. The functions $Q_{\lambda-1/2}^{(1,2)}(\cos\theta)$ are the travelling-wave Legendre functions, defined by (Nussenzveig 1965, equation (C.1))

$$Q_\nu^{(1,2)}(\cos\theta) \equiv \tfrac{1}{2}[P_\nu(\cos\theta) \pm (2\mathrm{i}/\pi)Q_\nu(\cos\theta)] \tag{2.9}$$

where P_ν and Q_ν are Legendre functions of the first and second kind, respectively. The path of integration is shown in figure 1: $\bar{\sigma}\infty$ denotes a direction in the second quadrant of the λ plane to the left of the curve h_{-2}, where the zeros of $H_\lambda^{(2)}(\beta)$ are located. The last expression in (2.7) explicitly exhibits the regularity of the representation at $\theta = \pi$ (where $Q_{\lambda-1/2}^{(1)}(\cos\theta)$ is singular).

The surface-wave amplitude $F_{\mathrm{s}}(\beta,\theta)$ is given by

$$F_{\mathrm{s}}(\beta,\theta) = -\frac{2\pi\mathrm{i}}{\beta}\sum_{n=1}^{\infty}\lambda_n r_n \frac{\exp(\mathrm{i}\pi\lambda_n)}{1+\exp(2\mathrm{i}\pi\lambda_n)}P_{\lambda_n-1/2}(-\cos\theta) \tag{2.10}$$

where λ_n are the poles of $S(\lambda,\beta)$ in the first quadrant of the λ plane (Regge poles), which are the roots of

$$H_{\lambda_n}^{(1)}(\beta) = 0 \tag{2.11}$$

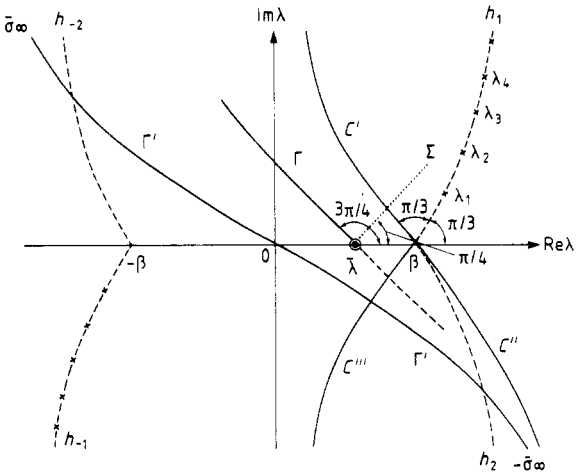

Figure 1. Paths of integration in the λ plane. The zeros of $H_\lambda^{(1)}(\beta)$ are asymptotically located on the curves h_1 and h_{-1}; those of $H_\lambda^{(2)}(\beta)$ on h_2 and h_{-2}. $\times\times\times$, Regge poles. $\odot$, saddle point $\bar{\lambda}$. Γ is the steepest-descent path through $\bar{\lambda}$ and Σ is the steepest-ascent one. The path Γ' is symmetrical about the origin.

arranged in order of increasing $|\lambda_n|$ (figure 1), and r_n is the residue of $S(\lambda, \beta)$ at λ_n,

$$r_n = -H_{\lambda_n}^{(2)}(\beta)/\dot{H}_{\lambda_n}^{(1)}(\beta) \tag{2.12}$$

where the dot denotes differentiation with respect to λ.

The representation (2.6) may be derived by applying the standard Watson transformation to (2.1), written in terms of $P_l(-\cos\theta) = (-1)^l P_l(\cos\theta)$. This yields

$$F(\beta, \theta) = \frac{1}{2\beta}\int_C [1 - S(\lambda, \beta)] P_{\lambda-1/2}(-\cos\theta)\frac{\lambda\, d\lambda}{\cos(\pi\lambda)}$$

where the path C runs from $\infty - i0$ to 0 and from 0 to $\infty + i0$, encircling the poles of the integrand at $\lambda = l + \frac{1}{2}(l = 0, 1, 2, \ldots)$.

The asymptotic behaviour of the integrand as $|\lambda| \to \infty$ is discussed in Nussenzveig (1965). We may deform C into the path Γ' shown in figure 1, leading to

$$F(\beta, \theta) = F_s(\beta, \theta) - \frac{1}{2\beta}\int_{\Gamma'} [1 - S(\lambda, \beta)] P_{\lambda-1/2}(-\cos\theta)\frac{\lambda\, d\lambda}{\cos(\pi\lambda)}$$

where F_s, given by (2.10), arises from the residues at the poles crossed in the path deformation.

The integrals associated with each of the two terms within square brackets (i.e. 1 and $S(\lambda, \beta)$) are separately convergent. The first one vanishes identically, because the integrand is odd ($P_{\lambda-1/2}(x) = P_{-\lambda-1/2}(x)$) and Γ' is taken to be symmetrical about the origin. In the second integral, we substitute the relation (Nussenzveig 1965, equation (C.5))

$$P_{\lambda-1/2}(-\cos\theta) = i\, e^{-i\pi\lambda} P_{\lambda-1/2}(\cos\theta) - 2i\cos(\pi\lambda) Q_{\lambda-1/2}^{(1)}(\cos\theta).$$

The first term on the right-hand side again does not contribute, because it leads to an odd integrand ($\exp(-i\pi\lambda) S(\lambda, \beta) = \exp(i\pi\lambda) S(-\lambda, \beta)$). The last term yields the integral in (2.7), so that we recover (2.6).

For $0 \leqslant \theta < \pi$, we may employ the alternative exact representation, manifestly regular at $\theta = 0$ (Nussenzveig 1965, equation (9.78)),

$$F(\beta, \theta) = F_d(\beta, \theta) + F_e(\beta, \theta) + \tilde{F}_s(\beta, \theta) \qquad 0 \leqslant \theta < \pi \tag{2.13}$$

where the diffraction amplitude $F_d(\beta, \theta)$ is given by

$$F_d(\beta, \theta) = \frac{i}{\beta} \int_0^\beta P_{\lambda - 1/2}(\cos\theta)\lambda \, d\lambda - \frac{2i}{\beta} \int_0^{i\infty} \frac{\exp(2i\pi\lambda)}{1 + \exp(2i\pi\lambda)} P_{\lambda - 1/2}(\cos\theta)\lambda \, d\lambda \tag{2.14}$$

which does not depend on $S(\lambda, \beta)$.

The edge amplitude $F_e(\beta, \theta)$ in (2.13) is given by

$$F_e(\beta, \theta) = F_{e-}(\beta, \theta) + F_{e+}(\beta, \theta) \tag{2.15}$$

where the below-edge amplitude F_{e-} is given by

$$F_{e-}(\beta, \theta) = -\frac{i}{\beta} \int_{i\infty}^{\beta} S(\lambda, \beta) P_{\lambda - 1/2}(\cos\theta)\lambda \, d\lambda \tag{2.16}$$

taken over a path of integration (typically represented by C' in figure 1) that stays to the left of the poles λ_n. The above-edge amplitude F_{e+} is given by

$$F_{e+}(\beta, \theta) = \frac{i}{\beta} \int_\beta^\infty [1 - S(\lambda, \beta)] P_{\lambda - 1/2}(\cos\theta)\lambda \, d\lambda. \tag{2.17}$$

Finally, the surface-wave amplitude $\tilde{F}_s(\beta, \theta)$ in (2.13) is given by

$$\tilde{F}_s(\beta, \theta) = -\frac{2\pi}{\beta} \sum_{n=1}^{\infty} \lambda_n r_n \frac{\exp(2i\pi\lambda_n)}{1 + \exp(2i\pi\lambda_n)} P_{\lambda_n - 1/2}(\cos\theta). \tag{2.18}$$

The names we have given to the various amplitudes will later be justified by their physical interpretation.

We now show explicitly the equivalence between the representations (2.6) and (2.13) at an arbitrary angle θ, $0 < \theta < \pi$. The proof (which differs slightly from that given in Nussenzveig (1965)) also provides the mechanism that guarantees smooth matching between the uniform and outer approximations at sufficiently large θ (cf § 6).

For this purpose, in (2.16) and (2.17), we employ the decomposition (cf (2.9))

$$P_{\lambda - 1/2}(\cos\theta) = Q^{(1)}_{\lambda - 1/2}(\cos\theta) + Q^{(2)}_{\lambda - 1/2}(\cos\theta) \tag{2.19}$$

leading to the corresponding decomposition

$$F_{e\pm}(\beta, \theta) = F^{(1)}_{e\pm}(\beta, \theta) + F^{(2)}_{e\pm}(\beta, \theta). \tag{2.20}$$

We also define

$$F^{(j)}_e(\beta, \theta) = F^{(j)}_{e+}(\beta, \theta) + F^{(j)}_{e-}(\beta, \theta) \qquad j = 1, 2 \tag{2.21}$$

so that (2.15) may be rewritten as

$$F_e(\beta, \theta) = F^{(1)}_e(\beta, \theta) + F^{(2)}_e(\beta, \theta). \tag{2.22}$$

From (2.17), we have

$$F^{(2)}_e(\beta, \theta) = -\frac{i}{\beta} \int_{i\infty}^{\beta} Q^{(2)}_{\lambda - \frac{1}{2}}(\cos\theta)\lambda \, d\lambda + \frac{i}{\beta} \left(\int_{i\infty}^{\beta} + \int_\beta^x \right) [1 - S(\lambda, \beta)] Q^{(2)}_{\lambda - 1/2}(\cos\theta)\lambda \, d\lambda \tag{2.23}$$

where the first (convergent) integral has been added and subtracted. It follows from Nussenzveig (1965, appendices A and C) that the path of integration in the last term of (2.23) may be closed at infinity, yielding a residue series at the poles λ_n (more precisely, as discussed in Nussenzveig (1965, § IV), one should take a sequence of paths passing halfway between the poles). Adding up (2.18), we get

$$F_e^{(2)}(\beta,\theta)+\tilde{F}_s(\beta,\theta)=-\frac{i}{\beta}\int_{i\infty}^{\beta}Q_{\lambda-1/2}^{(2)}(\cos\theta)\lambda\,d\lambda$$
$$+\frac{2\pi}{\beta}\sum_{n=1}^{\infty}\lambda_n r_n\left(Q_{\lambda_n-1/2}^{(2)}(\cos\theta)-\frac{\exp(2i\pi\lambda_n)}{1+\exp(2i\pi\lambda_n)}P_{\lambda_n-1/2}(\cos\theta)\right). \qquad (2.24)$$

According to Nussenzveig (1965, equation (C.5)), the last term of (2.24) is identical to (2.10), so that

$$F_e^{(2)}(\beta,\theta)+\tilde{F}_s(\beta,\theta)=-\frac{i}{\beta}\int_{i\infty}^{\beta}Q_{\lambda-1/2}^{(2)}(\cos\theta)\lambda\,d\lambda+F_s(\beta,\theta). \qquad (2.25)$$

On the other hand (cf (2.17)),

$$F_{e+}^{(1)}(\beta,\theta)=\frac{i}{\beta}\int_{\beta}^{-\bar{\sigma}\infty}[1-S(\lambda,\beta)]Q_{\lambda-1/2}^{(1)}(\cos\theta)\lambda\,d\lambda \qquad (2.26)$$

where we have shifted the path of integration from the real axis to the path C'' shown in figure 1. This is allowed, since the integrand is regular in between and decreases faster than exponentially at infinity. Taking into account (2.21) and (2.16), we get

$$F_e^{(1)}(\beta,\theta)=\frac{i}{\beta}\int_{\beta}^{-\bar{\sigma}\infty}Q_{\lambda-1/2}^{(1)}(\cos\theta)\lambda\,d\lambda$$
$$-\frac{i}{\beta}\left(\int_{i\infty}^{\beta}+\int_{\beta}^{-\bar{\sigma}\infty}\right)S(\lambda,\beta)Q_{\lambda-1/2}^{(1)}(\cos\theta)\lambda\,d\lambda \qquad (2.27)$$

where we have separated out the first (convergent) integral.

The path of integration in the last term is the path $C'+C''$ in figure 1, which is equivalent to the path Γ' from $\bar{\sigma}\infty$ to $-\bar{\sigma}\infty$. Thus, comparing with (2.7), we find

$$F_e^{(1)}(\beta,\theta)=F_r(\beta,\theta)+\frac{i}{\beta}\int_{\beta}^{-i\infty}Q_{\lambda-1/2}^{(1)}(\cos\theta)\lambda\,d\lambda \qquad (2.28)$$

where we have shifted the path in the last integral to the path C''' shown in figure 1.

From (2.22), (2.25) and (2.28), we obtain

$$F_e(\beta,\theta)+\tilde{F}_s(\beta,\theta)=F_r(\beta,\theta)+F_s(\beta,\theta)$$
$$-\frac{i}{\beta}\int_0^{\beta}[Q_{\lambda-1/2}^{(1)}(\cos\theta)+Q_{\lambda-1/2}^{(2)}(\cos\theta)]\lambda\,d\lambda$$
$$+\frac{i}{\beta}\int_0^{i\infty}Q_{\lambda-1/2}^{(2)}(\cos\theta)\lambda\,d\lambda+\frac{i}{\beta}\int_0^{-i\infty}Q_{\lambda-1/2}^{(1)}(\cos\theta)\lambda\,d\lambda \qquad (2.29)$$

where we have deformed C' and C'' into paths running from $\pm i\infty$ to 0 along the imaginary axis and from 0 to β. Changing λ to $-\lambda$ in the last integral and adding

together (2.29) and (2.14), we finally get, with the help of (2.13) and (2.19),

$$F(\beta,\theta)=F_r(\beta,\theta)+F_s(\beta,\theta)+\int_0^{i\infty}\Big(Q^{(2)}_{\lambda-1/2}(\cos\theta)+Q^{(1)}_{-\lambda-1/2}(\cos\theta)$$

$$-2\frac{\exp(2i\pi\lambda)}{1+\exp(2i\pi\lambda)}P_{\lambda-1/2}(\cos\theta)\Big)\lambda\,d\lambda. \tag{2.30}$$

According to Nussenzveig (1965, equations (C.4) and (C.5)), the integrand of the last integral is identically zero, so that we recover (2.6), thus completing the proof that the two representations are equivalent for $0<\theta<\pi$.

3. Outer approximation

For large enough θ (cf (3.9)),we may employ the 'outer' representation (2.6). We now derive asymptotic approximations to each of the two terms in (2.6) for large β.

3.1. WKB expansion of the reflection amplitude

Taking $\theta<\pi$ in the first representation (2.7), we set

$$\lambda=\beta\cos\psi \tag{3.1}$$

and we employ the Debye asymptotic expansion (A1.10) of $H^{(1,2)}_\lambda(\beta)$ in (2.8), as well as the asymptotic expansion (A1.15) for $Q^{(1)}_{\lambda-1/2}(\cos\theta)$. The result is

$$F_r(\beta,\theta)=e^{i\pi/4}\left(\frac{\beta}{2\pi\sin\theta}\right)^{1/2}\int_{\Gamma'_\psi}A(\psi,\theta,\beta)\exp[2i\beta\delta(\psi,\theta)]\,d\psi \tag{3.2}$$

where

$$\delta(\psi,\theta)=(\psi-\tfrac{1}{2}\theta)\cos\psi-\sin\psi \tag{3.3}$$

$$A(\psi,\theta,\beta)=\sin\psi(\cos\psi)^{1/2}\Big[1+\frac{i(d+\cot\theta)}{8\beta\cos\psi}$$

$$+\frac{1}{128\beta^2\cos^2\psi}\left(1-d^2-2d\cot\theta-\frac{9}{\sin^2\theta}\right)+\ldots\Big] \tag{3.4}$$

$$d\equiv 2\cot\psi(1+\tfrac{5}{3}\cot^2\psi) \tag{3.5}$$

and the path Γ'_ψ is the image of Γ' (figure 1) in the ψ plane. The terms of order λ^{-2} in the Debye asymptotic expansion of $H^{(1,2)}_\lambda(\beta)$, which are not written down in (A1.10), need not be included, because they are the same for $H^{(1)}_\lambda(\beta)$ and $H^{(2)}_\lambda(\beta)$, and they therefore cancel out in the ratio (2.8). Thus, (3.4) includes all corrections of order λ^{-2}.

The exponent in (3.2) has a saddle point at

$$\bar\psi=\tfrac{1}{2}\theta \tag{3.6}$$

corresponding, by (3.1), to

$$\bar\lambda=\beta\cos(\tfrac{1}{2}\theta)=k\bar b \tag{3.7}$$

where $\bar b=a\cos(\frac{1}{2}\theta)$ is the impact parameter of an incident ray that, after geometrical reflection at the surface, emerges in the direction θ. The steepest-descent path through

the saddle point crosses the real axis at an angle of $-\frac{1}{4}\pi$ both in the λ plane (path Γ in figure 1) and in the ψ plane.

Applying the saddle-point method to (3.2), we get the WKB expansion

$$F_r(\beta, \theta) = -\frac{1}{2}\left(1 + \frac{\mathrm{i}}{2\beta \sin^3 \frac{1}{2}\theta} + \frac{(2+3\cos^2 \frac{1}{2}\theta)}{(2\beta \sin^3 \frac{1}{2}\theta)^2} + \mathrm{O}[(2\beta \sin^3 \tfrac{1}{2}\theta)^{-3}]\right) \exp(-2\mathrm{i}\beta \sin \tfrac{1}{2}\theta) \tag{3.8}$$

which arises from geometrical reflection at the surface, justifying the name given to this amplitude. The first-order WKB correction agrees with that found by Keller *et al* (1956) by direct application of the WKB method. They also derived the second-order correction for $\theta = \pi$ and (3.8) agrees with their result, but we have not found a previous evaluation for general θ. Since the first-order correction is purely imaginary, the contribution from the second-order one to the differential cross section is of equal importance, so that it must be included for consistency.

It is clear by inspection of (3.8) that the domain of useful application of the WKB series as an asymptotic expansion for large β is

$$\theta \geqslant 2\gamma \tag{3.9}$$

where γ is defined by (1.2). This also follows from the breakdown of the Debye asymptotic expansions (A1.10) employed in (3.2) when $\beta - \bar{\lambda} = \mathrm{O}(\gamma^{-1})$, with $\bar{\lambda}$ given by (3.7).

The asymptotic expansion (A1.15), also employed in (3.2), breaks down when $\pi - \theta = \mathrm{O}(\lambda^{-1/2})$ so that, from (3.7), one would get the additional requirement $\pi - \theta \gg \beta^{-1/2}$. However, (3.8) is regular at $\theta = \pi$. As shown in Nussenzveig (1965, § IXC), an analysis based on the last representation in (2.7) and the uniform asymptotic expansion (A1.11) of $P_{\lambda-1/2}(-\cos\theta)$ confirms that (3.8) remains valid up to and including $\theta = \pi$.

3.2. Surface-wave amplitude

As was shown in Nussenzveig (1965), only the lowest-order Regge poles λ_n, located in the neighbourhood of $\lambda = \beta$ (figure 1), give a significant contribution to (2.10). The asymptotic expansion of these roots of (2.11) for large β is (Streifer and Kodis 1964)

$$\lambda_n = \beta + \exp(\mathrm{i}\pi/3)x_n\gamma^{-1} + \exp(2\mathrm{i}\pi/3)\frac{x_n^2}{60}\gamma + \frac{x_n^3}{1400}\left(1 - \frac{10}{x_n^3}\right)\gamma^3 + \mathrm{O}(\gamma^5) \tag{3.10}$$

where x_n is the nth zero of the Airy function $\mathrm{Ai}(-x)$,

$$\mathrm{Ai}(-x_n) = 0 \qquad n = 1, 2, \ldots . \tag{3.11}$$

The corresponding residues r_n, given by (2.12), can be obtained from Schöbe's asymptotic expansions for the Hankel functions (Nussenzveig 1969, appendix A). The result is

$$r_n = \frac{\exp(-\mathrm{i}\pi/6)}{2\pi a_n'^2 \gamma}[1 + \tfrac{1}{30}x_n \exp(\mathrm{i}\pi/3)\gamma^2 - \tfrac{3}{1400}3x_n^2 \exp(2\mathrm{i}\pi/3)\gamma^4 + \mathrm{O}(\gamma^6)] \tag{3.12}$$

where

$$a_n' \equiv \mathrm{Ai}(-x_n). \tag{3.13}$$

In particular, $x_1 = 2.338\ 10$, $x_2 = 4.087\ 95$, $a_1' = 0.701\ 21$, $a_2' = -0.803\ 11$ (for tables of x_n and a_n', see Abramowitz and Stegun (1964, p 478)). The results (3.10) and (3.12) agree with those found by Senior (1965) (see also Sengupta (1969, equation (10.58)): the expression given in these references is for $\lambda_n r_n$).

Finally, employing the uniform approximation (A1.11) for $P_{\lambda_n - 1/2}(-\cos\theta)$, (2.10) becomes

$$F_s(\beta, \theta) = -\frac{2\pi i}{\beta} \sum_n \lambda_n r_n \frac{\exp(i\pi\lambda_n)}{1+\exp(2i\pi\lambda_n)} \mathscr{P}(\pi - \theta, \lambda_n) \tag{3.14}$$

where $\mathscr{P}(\theta, \lambda)$ is defined by (A1.12), and λ_n and r_n are given by (3.10) and (3.12), respectively.

In particular, for $\pi - \theta \gg \beta^{-1}$, (A1.14) goes over into (A1.15) (cf (2.19)) and the dominant terms in (3.14) become

$$F_s(\beta, \theta) \approx \tfrac{1}{2} \exp(-5i\pi/12) \left(\frac{\gamma}{\pi \sin\theta}\right)^{1/2} \exp(i\beta\theta)$$
$$\times \sum_n a_n'^{-2} \exp[-\tfrac{1}{2}(\sqrt{3} - i) x_n \theta/\gamma] \qquad \pi - \theta \gg \beta^{-1} \tag{3.15}$$

in agreement with Nussenzveig (1965, equation (9.5)). The physical interpretation of the surface-wave contributions was discussed in Nussenzveig (1965): (3.15) shows the characteristic 'creeping-wave' decay with θ, becoming exponentially small for $\theta \gg \gamma$. It is also clear that the summation may be restricted to the lowest values of n. As θ decreases, approaching the lower bound (3.9) for the applicability of the outer approximation, (3.14) can give a significant correction to (3.8), which must be taken into account.

4. Uniform approximation: surface waves and diffraction

4.1. Surface-wave amplitude

By applying to (2.18) the same approximations that were applied to (2.10), we obtain

$$\tilde{F}_s(\beta, \theta) = -\frac{2\pi}{\beta} \sum_n \lambda_n r_n \frac{\exp(2i\pi\lambda_n)}{1+\exp(2i\pi\lambda_n)} \mathscr{P}(\theta, \lambda_n) \tag{4.1}$$

where λ_n and r_n are given by (3.10) and (3.12), respectively.

The dominant terms in (4.1) for $\theta \gg \beta^{-1}$ are similar to (3.15), except for the replacement of θ by $2\pi - \theta$. Thus, $\tilde{F}_s(\beta, \theta)$ represents the contribution from surface waves that have already taken at least half a turn around the sphere, which is exponentially small and can usually be neglected, except possibly at the lowest values of β for which the approximation is applicable.

4.2. Diffraction amplitude

The contribution (2.14), which depends on the scatterer only through its radius, may be regarded as defining 'diffraction scattering' in complex angular-momentum theory.

For a uniform asymptotic evaluation of the first integral in (2.14) when $\beta \gg 1$, we substitute $P_{\lambda - 1/2}(\cos\theta)$ by its uniform asymptotic expansion (A1.11), omitting the $O(\lambda^{-2})$ correction, which would give rise to a divergent integral at $\lambda = 0$ (where the

asymptotic expansion does not hold). The integrals that arise from the remaining terms are well known, yielding the result

$$\int_0^{\beta} P_{\lambda-1/2}(\cos\theta)\lambda\,\mathrm{d}\lambda \approx \beta(\theta/\sin\theta)^{1/2}\left[\frac{J_1(\beta\theta)}{\theta}-\frac{1}{8}\left(\frac{1}{\theta}-\cot\theta\right)\left(\frac{1-J_0(\beta\theta)}{\beta\theta}\right)\right]. \tag{4.2}$$

The first term of (4.2) differs from the well known Airy diffraction pattern only by the replacement of $\sin\theta$ by θ (van de Hulst 1957, §§ 8.31 and 12.32). At $\theta=0$, the RHS of (4.2) becomes $\frac{1}{2}\beta^2$, which is the exact result.

To evaluate the last integral in (2.14) for $\beta \gg 1$, we again approximate $P_{\lambda-1/2}(\cos\theta)$ by (A1.11) (with the $O(\lambda^{-2})$ terms omitted). We then replace $J_0(\lambda\theta)$ and $J_1(\lambda\theta)$ by their power series expansions and integrate term by term. With the change of variable $2\pi\lambda = \mathrm{i}x$, and employing the integral (Abramowitz and Stegun 1964, p 807)

$$\int_0^{\infty} \frac{x^{2n+1}}{\mathrm{e}^x+1}\,\mathrm{d}x = \frac{(2\pi)^{2n+2}}{4(n+1)}(1-1/2^{2n+1})|B_{2n+2}| \qquad n=0,1,2,\ldots \tag{4.3}$$

where B_n is the nth Bernoulli number, we find

$$\int_{\mathrm{i}\infty}^{0} \frac{\exp(2\mathrm{i}\pi\lambda)}{1+\exp(2\mathrm{i}\pi\lambda)} P_{\lambda-1/2}(\cos\theta)\lambda\,\mathrm{d}\lambda \approx \tfrac{1}{4}(\theta/\sin\theta)^{1/2} \times \sum_{n=0}^{\infty}\left(1-\frac{1}{2^{2n+1}}\right)\frac{|B_{2n+2}|}{(n+1)(n!)^2}\left(1+\frac{(1-\theta\cot\theta)}{16(n+1)}\right)\left(\frac{\theta}{2}\right)^n \tag{4.4}$$

which is a rapidly convergent series in the range of interest. For $\theta \neq 0$, it suffices to keep the first few terms; for $\theta = 0$, the result is exact.

Substituting (4.2) and (4.4) into (2.14), we finally obtain

$$F_{\mathrm{d}}(\beta,\theta) = \mathrm{i}\left(\frac{\theta}{\sin\theta}\right)^{1/2}\left[\frac{J_1(\beta\theta)}{\theta}-\frac{1}{8}\left(\frac{1}{\theta}-\cot\theta\right)\left(\frac{1-J_0(\beta\theta)}{\beta\theta}\right) + \frac{1}{24\beta}\left(1+\frac{31}{120}\left(\frac{\theta}{2}\right)^2+\frac{53}{1008}\left(\frac{\theta}{2}\right)^4+\ldots\right)\right]. \tag{4.5}$$

In particular, for $\theta = 0$, this reduces to the exact result

$$F_{\mathrm{d}}(\beta,0) = \mathrm{i}\tfrac{1}{2}\beta(1+1/12\beta^2). \tag{4.6}$$

5. Uniform approximation: above-edge amplitude

In terms of a ray picture, the integral (2.17) represents the contribution from incident rays with impact parameters $\lambda/k \geqslant a$. Correspondingly, for $\lambda/k \gg a$, the integrand decreases faster than exponentially (Nussenzveig 1969, figure 18), and the only significant contribution arises from the upper-edge domain (Nussenzveig 1969, equation (1.14))

$$\lambda-\beta = \gamma^{-1}x \qquad x = O(1) \tag{5.1}$$

justifying the name 'above-edge amplitude' (cf also van de Hulst 1957, § 17.2).

From (2.8) and the uniform asymptotic expansions (A1.1) and (A1.2) of $H_\lambda^{(1,2)}(\beta)$ for $\lambda \geqslant \beta$, we find

$$1-S(\lambda,\beta) \equiv 2J_\lambda(\beta)/H_\lambda^{(1)}(\beta) \approx \exp(\mathrm{i}\pi/3)H_+(x,\varphi) \tag{5.2}$$

where

$$\lambda = \beta \cosh \varphi \tag{5.3}$$

$$x \equiv [\tfrac{3}{2}\beta(\varphi \cosh \varphi - \sinh \varphi)]^{2/3} \tag{5.4}$$

and we have introduced the notation

$$H_+(x, \varphi) \equiv \frac{\mathrm{Ai}(x) - \exp(\mathrm{i}\pi/6)\sigma_+(x, \varphi)\mathrm{Ai}'(x)}{\mathrm{Ai}(\exp(2\mathrm{i}\pi/3)x) + \exp(-\mathrm{i}\pi/6)\sigma_+(x, \varphi)\mathrm{Ai}'(\exp(2\mathrm{i}\pi/3)x)} \tag{5.5}$$

with

$$\sigma_+(x, \varphi) \equiv \frac{5}{24\beta} \frac{\exp(-\mathrm{i}\pi/6)}{\sqrt{x} \sinh \varphi} (L_+(\varphi) + \tfrac{3}{5}) \tag{5.6}$$

$$L_+(\varphi) \equiv [3(\varphi \coth \varphi - 1)]^{-1} - \coth^2 \varphi. \tag{5.7}$$

In the coefficients of Ai and Ai′ in the numerator and denominator of (5.5), we have neglected higher-order $O(\lambda^{-2})$ corrections (cf (A1.1)). The Ai′ terms are corrections to the dominant Ai terms, so that (5.2) can be expanded in the form

$$1 - S(\lambda, \beta) = \exp(\mathrm{i}\pi/3) \frac{\mathrm{Ai}(x)}{\mathrm{Ai}(\exp(2\mathrm{i}\pi/3)x)} \left[1 + \frac{\sigma_+(x, \varphi)}{2\pi \mathrm{Ai}(x)\mathrm{Ai}(\exp(2\mathrm{i}\pi/3)x)} \right.$$
$$\left. + \exp(\mathrm{i}\pi/3) \left(\sigma_+(x, \varphi) \frac{\mathrm{Ai}'(\exp(2\mathrm{i}\pi/3)x)}{\mathrm{Ai}(\exp(2\mathrm{i}\pi/3)x)} \right)^2 + O(\lambda^{-3}) \right] \tag{5.8}$$

where we have employed the Wronskian relation (cf (A1.6) and (A1.7))

$$W[\mathrm{Ai}(z), \mathrm{Ai}(\exp(\pm 2\mathrm{i}\pi/3)z)] = (2\pi)^{-1} \exp(\mp \mathrm{i}\pi/6). \tag{5.9}$$

Note that $O(\lambda^{-2})$ correction terms to the coefficients of $\mathrm{Ai}(x)$, $\mathrm{Ai}(\exp(2\mathrm{i}\pi/3)x)$ would cancel out in this expansion. However, we will keep the more accurate expression (5.5), rather than the expansion (5.8), in the uniform approximation.

From the asymptotic expansion (A1.8) of $\mathrm{Ai}(z)$, we find that the dominant term in (5.8) for $x \gg 1$ is

$$1 - S(\lambda, \beta) \sim \mathrm{i} \exp(-\tfrac{4}{3}x^{3/2}) \qquad x \gg 1 \tag{5.10}$$

which decreases faster than exponentially with x (cf the beginning of this section). Taking into account the higher-order terms in (A1.8) and (A1.9), as well as (5.4), we find that (5.8), for $x \gg 1$, goes over into the Debye asymptotic expansion (the analogue of (A1.10) for $\lambda > \beta$), up to and including $O(\beta^{-2})$ correction terms.

Similarly, from (A1.11) and (5.3),

$$P_{\lambda - 1/2}(\cos \theta) \approx \mathscr{P}(\theta, \beta \cosh \varphi) \tag{5.11}$$

where $\mathscr{P}(\theta, \lambda)$ is defined by (A1.12).

Substituting (5.2) and (5.11) into (2.17), we get the desired uniform approximation of $F_{e+}(\beta, \theta)$. For actual numerical evaluation, the most convenient integration variable is x, the natural scale variable, which is $O(1)$ in the edge domain. By differentiating (5.3) and (5.4) we find

$$\mathrm{d}\lambda / \mathrm{d}x = \sqrt{x}/\varphi(x). \tag{5.12}$$

To express φ in terms of x, we must invert (5.4), with $x = O(1)$. The inversion is performed in appendix 2, with the result

$$\varphi(x) = \varphi_0[1 - \tfrac{1}{30}\varphi_0^2 + \tfrac{41}{12600}\varphi_0^4 - \tfrac{317}{1134000}\varphi_0^6 + O(\varphi_0^8)] \tag{5.13}$$

where

$$\varphi_0(x) \equiv \gamma\sqrt{x}. \tag{5.14}$$

Since γ is at most of order unity (for the lowest values of β) and $x = O(1)$ within the effective range of integration, (5.13) is rapidly convergent. For $\beta \gg 1$, we have $\varphi_0 \ll 1$ within this range; to lowest order,

$$\lambda \approx \beta \cosh \varphi_0 \approx \beta(1 + \tfrac{1}{2}\varphi_0^2) = \beta + \gamma^{-1}x$$

(cf (5.1)).

Finally, substituting the above results into (2.17), we obtain the uniform approximation of the above-edge amplitude

$$F_{e+}(\beta, \theta) = -\exp(-i\pi/6)\int_0^\infty H_+(x, \varphi)\mathscr{P}(\theta, \beta\cosh\varphi)\varphi^{-1}\cosh\varphi\sqrt{x}\,dx. \tag{5.15}$$

The effective cutoff for the integral (cf (5.10)) is around $x \sim 4$ (cf (2.5)).

6. Uniform approximation: below-edge amplitude

In (2.16), we employ the uniform asymptotic expansion (A1.1) in the form (A1.3), leading to

$$S(\lambda, \beta) \equiv -H_\lambda^{(2)}(\beta)/H_\lambda^{(1)}(\beta) \approx \exp(-i\pi/3)H_-(x, \psi) \tag{6.1}$$

where

$$\lambda = \beta\cos\psi \tag{6.2}$$

$$x \equiv \exp(i\pi/3)[\tfrac{3}{2}\beta(\sin\psi - \psi\cos\psi)]^{2/3} \tag{6.3}$$

and we have introduced the notation

$$H_-(x, \psi) \equiv \frac{\mathrm{Ai}(x) - \exp(-i\pi/6)\sigma_-(x, \psi)\mathrm{Ai}'(x)}{\mathrm{Ai}(\exp(-2i\pi/3)x) + \exp(i\pi/6)\sigma_-(x, \psi)\mathrm{Ai}'(\exp(-2i\pi/3)x)} \tag{6.4}$$

with

$$\sigma_-(x, \psi) \equiv -\frac{5}{24\beta}\frac{\exp(-i\pi/3)}{\sqrt{x}\sin\psi}[L_-(\psi) + \tfrac{3}{5}] \tag{6.5}$$

$$L_-(\psi) \equiv [3(\psi\cot\psi - 1)]^{-1} + \cot^2\psi. \tag{6.6}$$

The analogue of (5.8) for (2.8) is the expansion

$$S(\lambda, \beta) = \exp(-i\pi/3)\frac{\mathrm{Ai}(x)}{\mathrm{Ai}(\exp(-2i\pi/3)x)}\left[1 + \frac{\sigma_-(x, \psi)}{2\pi\mathrm{Ai}(x)\mathrm{Ai}(\exp(-2i\pi/3)x)}\right.$$
$$\left. + \exp(i\pi/3)\left(\sigma_-(x, \psi)\frac{\mathrm{Ai}'(\exp(-2i\pi/3)x)}{\mathrm{Ai}(\exp(-2i\pi/3)x)}\right)^2 + O(\lambda^{-3})\right] \tag{6.7}$$

where we have employed (5.9). Also, from (A1.8), we find as the dominant term of (6.7), for $x \gg 1$,

$$S(\lambda, \beta) \sim -i \exp(-\tfrac{4}{3}x^{3/2}) \qquad x \gg 1 \tag{6.8}$$

and, taking into account (6.3) and higher-order terms in (A1.8) and (A1.9), we find that (6.7), for $x \gg 1$, goes over into the result given by the Debye asymptotic expansion (A1.10), up to and including $O(\beta^{-2})$ terms, the same ones that were employed in (3.4).

Similarly, from (A1.11) and (6.2),

$$P_{\lambda-1/2}(\cos\theta) \approx \mathcal{P}(\theta, \beta\cos\psi). \tag{6.9}$$

Since $P_{\lambda-1/2}(1) = 1$, the integrand of (2.16) at $\theta = 0$ is dominated by (6.8), so that, starting from $x = 0$ (equivalent to $\lambda = \beta$, by (6.2)), the direction of fastest decrease in the x plane is along the positive real axis. This is the reason for the choice of phase in (6.3) (cf Nussenzveig 1969, equation (4.66)). From (6.2) and (6.3), we find

$$d\lambda/dx = i\sqrt{x}/\psi(x). \tag{6.10}$$

The inversion of (6.3) to express ψ in terms of x for $x = O(1)$ is performed in appendix 2, yielding the analogues of (5.13) and (5.14),

$$\psi(x) = \psi_0[1 + \tfrac{1}{30}\psi_0^2 + \tfrac{41}{12600}\psi_0^4 + \tfrac{317}{1134000}\psi_0^6 + O(\psi_0^8)] \tag{6.11}$$

where

$$\psi_0(x) \equiv \exp(-i\pi/6)\gamma\sqrt{x}. \tag{6.12}$$

In particular, for $\beta \gg 1$ and $x = O(1)$, we have $|\psi_0(x)| \ll 1$, so that $\lambda = \beta\cos\psi \approx \beta(1 - \frac{1}{2}\psi_0^2)$, i.e.

$$\lambda \approx \beta + \exp(2i\pi/3)\gamma^{-1}x \qquad x = O(1). \tag{6.13}$$

Thus in the λ plane, the path C' of steepest decrease (at $\theta = 0$) leaves the real axis at an angle of $2\pi/3$, as shown in figure 1. Note, however, that (6.8) holds for $x \gg 1$, and that $\lambda = \beta$ is not a saddle point.

In a suitable neighbourhood of the forward direction, $0 \leqslant \theta \leqslant \theta_0$, where θ_0 will be determined below, this is a good choice for the path of integration. Substituting (6.1), (6.9) and (6.10) into (2.16), we obtain

$$F_{e-}(\beta, \theta) = -\exp(-i\pi/3)\int_0^c H_-(x, \psi)\mathcal{P}(\theta, \beta\cos\psi)\psi^{-1}\cos\psi\sqrt{x}\,dx \qquad 0 \leqslant \theta \leqslant \theta_0 \tag{6.14}$$

where c, the effective cutoff, is essentially the same as that for (5.15) for small enough θ.

What happens when θ increases? By (2.19) and (A1.15), we have, for $\theta\,\mathrm{Im}\,\lambda \gg 1$,

$$P_{\lambda-1/2}(\cos\theta) \sim Q^{(1)}_{\lambda-1/2}(\cos\theta) \approx \exp(-i\pi/4)\frac{\exp(-i\lambda\theta)}{(2\pi\lambda\sin\theta)^{1/2}} \tag{6.15}$$

which increases exponentially as λ moves up along C' in figure 1. Taking into account (6.8), we see that, for $|x| \geqslant 1$, the integrand of (6.14) is dominated by the exponential factor

$$\exp[\Phi(x, \beta, \theta)] \equiv \exp[-\tfrac{4}{3}x^{3/2} - i\beta\theta\cos\psi(x)] \tag{6.16}$$

where $\psi(x)$ is given by (6.11). This approximation may be applied for

$$|x| \geqslant 1 \qquad \frac{\theta}{2\gamma}|x| \geqslant 1. \tag{6.17}$$

According to (6.16), for $\theta \geqslant 2\gamma$, if we integrate (6.14) along the real x axis, the integrand has a peak at $x \approx (\theta/4\gamma)^2$, with a width of order $(\theta/2\gamma)^{1/2}$, so that the cutoff c would have to take on larger and larger values if we were to apply (6.14) beyond $\theta \sim 2\gamma$.

On the other hand, in (6.16),

$$\partial\Phi(x, \beta, \theta)/\partial x = \sqrt{x}(\theta/\psi - 2) \tag{6.18}$$

so that for complex x we find a saddle point at

$$\bar{\psi} = \psi(\bar{x}) = \tfrac{1}{2}\theta \tag{6.19}$$

i.e. by (6.3), at

$$\bar{x} = \exp(\mathrm{i}\pi/3)\bar{t} \qquad \bar{t} \equiv [\tfrac{3}{2}\beta(\sin\tfrac{1}{2}\theta - \tfrac{1}{2}\theta\cos\tfrac{1}{2}\theta)]^{2/3}. \tag{6.20}$$

In particular, for $\theta \ll 1$, (6.20) yields

$$\bar{t} = (\theta/2\gamma)^2[1 - \tfrac{1}{15}(\tfrac{1}{2}\theta)^2 + \mathrm{O}(\theta^4)] \qquad \theta \ll 1. \tag{6.21}$$

By comparing (6.19) with (3.6), we see that this is just the geometrical reflection saddle point of § 3.

In view of (6.17) and (6.21), we can say that the saddle point appears only for

$$\theta \geqslant 2\gamma \tag{6.22}$$

which is the same as (3.9), the condition for applicability of the outer approximation.

From (6.18) and (6.20), we obtain

$$\partial^2\Phi(\bar{x}, \beta, \theta)/\partial x^2 = 3^{2/3}\exp(5\mathrm{i}\pi/6)\gamma(\sin\tfrac{1}{2}\theta - \tfrac{1}{2}\theta\cos\tfrac{1}{2}\theta)^{2/3}/[(\tfrac{1}{2}\theta)^2\sin\tfrac{1}{2}\theta]$$
$$\sim (2\gamma/\theta)\exp(5\mathrm{i}\pi/6) \qquad \theta \ll 1 \tag{6.23}$$

so that the steepest-descent path in the neighbourhood of $\bar{x}$ is given by

$$x - \bar{x} = \exp(\mathrm{i}\pi/12)u \qquad \mathrm{Im}\, u = 0 \tag{6.24}$$

which, by (6.13), corresponds to the path Γ in the λ plane, meeting the real axis at $\bar{\lambda}$ at an angle of $3\pi/4$.

Figure 1 also shows, with a dotted line, the steepest-ascent path Σ through $\bar{\lambda}$ that crosses the real axis at an angle of $\frac{1}{4}\pi$. For $\theta \geqslant 2\gamma$, the path C' associated with (6.14) would have to 'climb up over the ridge' across Σ before 'coming down on the lowlands' on the other side (leading to the peaked behaviour discussed following (6.17)), so that it would not be a good path. This suggests taking $\theta_0 \leqslant 2\gamma$ in (6.14).

From (6.15) and (2.20), we see that the difficulties found for $\theta \geqslant 2\gamma$ affect only $F_{\mathrm{e}-}^{(1)}(\beta, \theta)$; by (A1.15), $Q_{\lambda-1/2}^{(2)}(\cos\theta)$ decays exponentially for $\mathrm{Im}\,\lambda > 0$, so that the analogue of (6.14) for $F_{\mathrm{e}-}^{(2)}(\beta, \theta)$ can still be employed for $\theta > \theta_0$:

$$F_{\mathrm{e}-}^{(2)}(\beta, \theta) = -\exp(-\mathrm{i}\pi/3)\int_0^c H_-(x, \psi)\mathscr{P}^{(2)}(\theta, \beta\cos\psi)$$
$$\times \psi^{-1}\cos\psi\sqrt{x}\,\mathrm{d}x \qquad \theta \geqslant \theta_0 \tag{6.25}$$

where $\mathscr{P}^{(2)}(\theta, \lambda)$ is defined by (A1.14).

Since $F_{\mathrm{e}-}^{(1)}(\beta, \theta)$ must eventually give rise to the WKB approximation at larger θ (cf (2.27)), a good path for $\theta > \theta_0$ should go through $\bar{\lambda}$ before joining up with (5.15) at $\lambda = \beta$. Thus for $F_{\mathrm{e}-}^{(1)}(\beta, \theta)$, $\theta > \theta_0$, instead of integrating over C' in figure 1, we first go from β to $\bar{\lambda}$ along the real-λ axis, which is equivalent to taking a stationary phase

path, and then we go into the upper half-plane along the steepest-descent path Γ from $\bar{\lambda}$. The equivalent path in the x plane follows from (6.20) and (6.24). The result is

$$F_{e-}^{(1)}(\beta, \theta) = \hat{F}_{e-}^{(1)}(\beta, \theta) + \tilde{F}_{e-}^{(1)}(\beta, \theta) \qquad \theta > \theta_0 \tag{6.26}$$

where

$$\hat{F}_{e-}^{(1)}(\beta, \theta) = -\exp(i\pi/6) \int_0^{\bar{t}} H_-(\exp(i\pi/3)t, \hat{\psi}) \mathscr{P}^{(1)}(\theta, \beta \cos \hat{\psi}) \times \hat{\psi}^{-1} \cos \hat{\psi} \sqrt{t}\, dt \tag{6.27}$$

with $\bar{t}$ defined by (6.20), $\mathscr{P}^{(1)}(\theta, \lambda)$ by (A1.14), and

$$\hat{\psi}(t) \equiv \psi(x = \exp(i\pi/3)t). \tag{6.28}$$

With $x = \exp(i\pi/3)t$, by (6.2) and (6.3), (6.27) represents the integral from β to $\bar{\lambda}$ along the real-λ axis (stationary phase path). Along this path (cf (6.12)), $\hat{\psi}$ is real and (cf (6.1)) $|H_-| = |S(\lambda, \beta)| = 1$.

The other term of (6.26) is

$$\tilde{F}_{e-}^{(1)}(\beta, \theta) = -\exp(-i\pi/4) \int_0^{u_0} H_-(z, \tilde{\psi}) \mathscr{P}^{(1)}(\theta, \beta \cos \tilde{\psi}) \tilde{\psi}^{-1} \cos \tilde{\psi} \sqrt{z}\, du \tag{6.29}$$

where

$$z(u) \equiv \bar{x} + \exp(i\pi/12)u \qquad \tilde{\psi}(u) \equiv \psi(z) \tag{6.30}$$

so that (6.29) represents the integral along the steepest-descent path (6.24), corresponding to the path Γ from $\bar{\lambda}$ into the upper half-plane in figure 1.

Along this path, by (6.23), the integrand decreases like $\exp(-u^2/\rho^2)$, where

$$\rho \equiv [2(\partial^2 \Phi(\bar{x}, \beta, \theta)/\partial x^2)^{-1}]^{1/2} \approx (\theta/\gamma)^{1/2} \qquad \theta \ll 1 \tag{6.31}$$

is the range of the saddle point. Thus the effective cutoff for the integral, which we have taken as the upper limit in (6.29), is

$$u_0 \equiv c'\rho \tag{6.32}$$

where c' is a numerical constant.

Since the integrands of (6.14), (6.25) and (6.29) decrease faster than exponentially, the effective cutoff constants c and c' (cf (6.32)) are numbers of order unity, the choice of which depends on the accuracy that one is aiming at; to reduce computing time, one wants to pick the lowest possible values. We must also choose θ_0, and the choices of these parameters must be such that the representations (6.14), and (6.25) and (6.26) (with F_{e-} given by (2.20)) match smoothly at $\theta = \theta_0$.

The difference between these representations is that, in the x plane, the integral associated with $F_{e-}^{(1)}(\beta, \theta)$ is taken from $x = 0$ to c in (6.14), whereas in (6.26) it is taken first from $x = 0$ to $\bar{x}$, corresponding to (6.27), and then from $x = \bar{x}$ to $\bar{x} + \exp(i\pi/12)u_0$, corresponding to (6.29). For smooth matching, by Cauchy's theorem, the integral joining the endpoints of these two alternative paths must be negligible, to the desired order of accuracy, at $\theta = \theta_0$. A convenient choice is

$$\theta_0 = \gamma \qquad c = 4 \qquad c' = 3.5. \tag{6.33}$$

These values were employed in the numerical tests discussed in § 9.

The least rapidly convergent term in the uniform approximation is the definite integral (6.27) along the stationary phase path. Since the range of the stationary phase

point is also given by (6.31), the dominant contributions to (6.27) arise from a neighbourhood (extending over a few times the range) of the upper limit and from the lower limit of integration (Bleistein and Handelsman 1975). The contribution from the lower limit is cancelled out by the corresponding contribution from (5.15), so that, for large θ, one half of the WKB result (3.8) arises from the stationary-phase contribution in (6.27) and the other half from the saddle-point contribution in (6.29).

Since all terms included in (3.2) are limiting forms of corresponding terms included in the uniform approximation, smooth matching with the outer approximation at large θ is guaranteed, following the lines of the matching mechanism discussed in § 2. This completes the proof that the approximation developed in §§ 4–6 is indeed uniform.

The extinction efficiency, according to (2.4) and (2.13), is given by

$$Q_{\text{ext}}(\beta) = 2 + \frac{1}{6\beta^2} - \frac{8\pi}{\beta^2}\,\text{Im}\left(\sum_n \lambda_n r_n \frac{\exp(2i\pi\lambda_n)}{1+\exp(2i\pi\lambda_n)}\right) + \frac{4}{\beta}\,\text{Re}\left(\exp(i\pi/6)\int_0^\infty H_-(x,\psi)\psi^{-1}\cos\psi\sqrt{x}\,dx + \exp(i\pi/3)\int_0^\infty H_+(x,\varphi)\varphi^{-1}\cosh\varphi\sqrt{x}\,dx\right) \tag{6.34}$$

where the first two terms arise from the diffraction amplitude (4.6), the next one from the surface-wave amplitude (4.1), and the last two from the above-edge and below-edge amplitudes (5.15) and (6.14) (where we have extended the upper limit to infinity).

7. The Fock approximation

Simplified versions of the uniform approximation may be useful, particularly for very large β and very small θ, or when less accurate results suffice. We now discuss them, establishing contact with previously known results, including the Fock approximation. These are all transitional approximations, holding only in narrow angular domains, that lead to severe patching problems when one tries to extend them to larger angles (cf § 9).

Since the main contribution to (5.15) arises from $x = O(1)$, one has $\varphi \ll 1$ in the relevant portion of the domain of integration when $\gamma \ll 1$. Thus, one may employ the power series expansion of cosh φ, together with (5.13), yielding

$$\beta\theta\cosh\varphi = \beta\theta + \theta x/\gamma + \tfrac{1}{60}\gamma\theta x^2 + \ldots \tag{7.1}$$

where the last term is small under the above conditions. Consequently, from (A1.12),

$$\mathcal{P}(\theta, \beta\cosh\varphi) \approx \left(\frac{\theta}{\sin\theta}\right)^{1/2}[J_0(\beta\theta + \theta x/\gamma) - \tfrac{1}{60}\gamma\theta x^2 J_1(\beta\theta + \theta x/\gamma)]. \tag{7.2}$$

Similarly, from (5.6) and (5.7),

$$\sigma_+(x,\varphi) \approx -\tfrac{1}{140}\exp(-i\pi/6)\gamma^4 \tag{7.3}$$

so that, from (5.2) and (5.8),

$$H_+(x,\varphi) \approx \frac{\text{Ai}(x)}{\text{Ai}(\exp(2i\pi/3)x)}[1 + O(\gamma^4)]. \tag{7.4}$$

Finally, under the same conditions, (5.13) and (5.14) yield

$$\varphi^{-1}\cosh\varphi\sqrt{x}=\gamma^{-1}[1+\tfrac{8}{15}\gamma^2x+O(\gamma^4x^2)]. \tag{7.5}$$

Substituting (7.2), (7.4) and (7.5) into (5.15), we obtain

$$F_{e+}(\beta,\theta)\approx-\frac{\exp(-i\pi/6)}{\gamma}\left(\frac{\theta}{\sin\theta}\right)^{1/2}\int_0^\infty dx\frac{\mathrm{Ai}(x)}{\mathrm{Ai}(\exp(2i\pi/3)x)}$$
$$\times[(1+\tfrac{8}{15}\gamma^2x)J_0(\beta\theta+\theta x/\gamma)-\tfrac{1}{60}\gamma\theta x^2J_1(\beta\theta+\theta x/\gamma)]. \tag{7.6}$$

Applying equivalent approximations to (6.14), we get

$$F_{e-}(\beta,\theta)\approx-\frac{\exp(-i\pi/6)}{\gamma}\left(\frac{\theta}{\sin\theta}\right)^{1/2}\int_0^\infty dx\frac{\mathrm{Ai}(x)}{\mathrm{Ai}(\exp(-2i\pi/3)x)}$$
$$\times[(1+\tfrac{8}{15}\exp(2i\pi/3)\gamma^2x)J_0(\beta\theta+(\theta/\gamma)\exp(2i\pi/3)x)$$
$$+\tfrac{1}{60}\gamma\theta\exp(i\pi/3)x^2J_1(\beta\theta+(\theta/\gamma)\exp(2i\pi/3)x)] \qquad 0\leqslant\theta\leqslant\theta_0. \tag{7.7}$$

From (2.15), (7.6) and (7.7), we find

$$F_e(\beta,\theta)\approx\frac{i}{\gamma}\left(\frac{\theta}{\sin\theta}\right)^{1/2}[\mathscr{F}_{0,0}(\beta,\theta)+\tfrac{8}{15}\gamma^2\mathscr{F}_{1,0}(\beta,\theta)$$
$$-\tfrac{1}{60}\gamma\theta\mathscr{F}_{2,1}(\beta,\theta)] \qquad 0\leqslant\theta\leqslant\theta_0 \qquad \gamma\ll1 \tag{7.8}$$

where

$$\mathscr{F}_{m,n}(\beta,\theta)\equiv\exp(i\pi/3)\int_0^\infty\frac{x^m\mathrm{Ai}(x)}{\mathrm{Ai}(\exp(2i\pi/3)x)}J_n(\beta\theta+\theta x/\gamma)\,dx$$
$$+\exp[i(2m+1)\pi/3]\int_0^\infty\frac{x^m\mathrm{Ai}(x)}{\mathrm{Ai}(\exp(-2i\pi/3)x)}$$
$$\times J_n(\beta\theta+(\theta/\gamma)\exp(2i\pi/3)x)\,dx \tag{7.9}$$

are generalised Fock functions of 'reflection coefficient type' (Logan 1959, Logan and Yee 1962, Nussenzveig 1969, equation (4.64)).

In appendix 3, we reduce the above expressions to generalised Fock functions, defined by (Nussenzveig 1969, equation (4.67))

$$F_{m,n}(\beta,\theta)\equiv\frac{\exp(i\pi/6)}{2\pi}\left(\int_{\exp(2i\pi/3)\infty}^0+\int_0^\infty\right)\frac{z^mJ_n(\beta\theta+\theta z/\gamma)}{\mathrm{Ai}^2(\exp(2i\pi/3)z)}\,dz. \tag{7.10}$$

The result is

$$F_e(\beta,\theta)\approx i\left(\frac{\theta}{\sin\theta}\right)^{1/2}\left(-\frac{J_1(\beta\theta)}{\theta}+\frac{1}{\theta}F_{0,1}(\beta,\theta)\right.$$
$$\left.+\frac{\gamma^2}{2\theta}F_{1,1}(\beta,\theta)+\tfrac{1}{60}\gamma F_{2,0}(\beta,\theta)\right) \qquad 0\leqslant\theta\leqslant\gamma\ll1 \tag{7.11}$$

which agrees with the impenetrable sphere limit of Nussenzveig (1969, equation (4.68)). In (7.11), we have taken $\theta_0=\gamma$, as in (6.33).

For $\theta \ll \gamma$, we can expand $F_{m,n}(\beta, \theta)$ into powers of θ/γ (Nussenzveig 1969, equation (4.74)) and (7.11) becomes

$$F_e(\beta, \theta) = i\left(\frac{\theta}{\sin\theta}\right)^{1/2}\left\{\left[\frac{M_0}{\gamma}+\frac{8}{15}M_1\gamma-\frac{M_2}{2\gamma}\left(\frac{\theta}{\gamma}\right)^2+\ldots\right]J_0(\beta\theta)\right.$$

$$\left.-(M_1/\gamma+\tfrac{3}{10}M_2\gamma+\ldots)(\theta/\gamma)J_1(\beta\theta)+\ldots\right\} \qquad 0\leqslant\theta\ll\gamma\ll 1 \qquad (7.12)$$

which agrees with the impenetrable sphere limit of Nussenzveig (1969, equation (4.75)) to the order of accuracy computed there. In (7.12),

$$M_m \equiv \mathcal{F}_{m,0}(\beta, 0) = \exp(i\pi/3)\int_0^\infty \frac{\mathrm{Ai}(x)}{\mathrm{Ai}(\exp(2i\pi/3)x)}x^m\,dx$$

$$+\exp[i(2m+1)\pi/3]\int_0^\infty \frac{\mathrm{Ai}(x)}{\mathrm{Ai}(\exp(-2i\pi/3)x)}x^m\,dx \qquad (7.13)$$

which is equivalent to the definition of these coefficients given by Wu (1956). In particular (Lisle *et al* 1985)

$$M_0 = 1.255\,124\,56\exp(i\pi/3) \qquad M_1 = 0.532\,2907\exp(2i\pi/3)$$

$$M_2 = 0.067\,717. \qquad (7.14)$$

From (2.4), (4.6) and (7.12), the extinction efficiency becomes

$$Q_{ext}(\beta) = 2+2\,\mathrm{Re}[M_0\gamma^2+\tfrac{8}{15}M_1\gamma^4+(\tfrac{4}{175}M_2+\tfrac{23}{1680})\gamma^6+O(\gamma^8)] \qquad \gamma\ll 1 \qquad (7.15)$$

where the surface-wave contribution (4.1) to (2.13) has been neglected, as it is exponentially small for $\gamma \ll 1$. The term $\frac{23}{1680}$ in (7.15) differs by a factor $\frac{1}{4}$ from the corresponding term in Wu (1956).

8. Physical interpretation

8.1. Relationship with semiclassical dynamics

The 'crude semiclassical approximation' to $F(\beta, \theta)$ for our problem is given by (Berry 1969)

$$F_{sc}(\beta, \theta) = -\frac{i}{\beta}\left(\frac{\bar{\lambda}}{\sin\theta|\Theta'(\bar{\lambda})|}\right)^{1/2}\exp[iS(\bar{\lambda})] \qquad (8.1)$$

where $\Theta(\lambda)$ is the classical deflection function associated with the impact parameter λ/k, given by the well known billiard-ball expression

$$\Theta(\lambda) = \begin{cases} 2\cos^{-1}(\lambda/\beta) & \lambda/k \leqslant a \\ 0 & \lambda/k \geqslant a \end{cases} \qquad (8.2)$$

which is plotted in figure 2. The function $S(\lambda)$ is the classical action along the

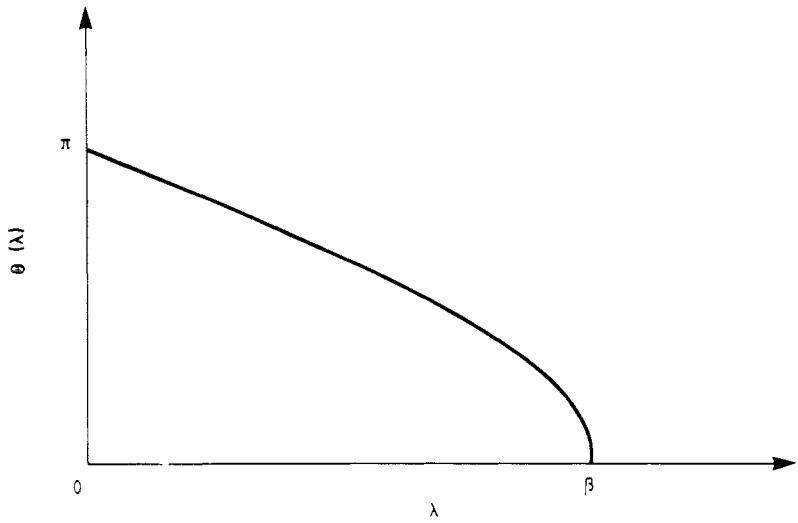

Figure 2. Classical deflection function (equation (8.2)).

corresponding (geometrical reflection) path, given by

$$S(\lambda) = 2[\lambda \cos^{-1}(\lambda/\beta) - (\beta^2 - \lambda^2)^{1/2} - \pi/4] - \lambda\Theta(\lambda) \qquad 0 \leq \lambda \leq \beta \tag{8.3}$$

where the expression within square brackets is the WKB phase shift (cf (2.8) and (A1.10)). Finally, in (8.1), $\bar{\lambda}$ is the stationary phase point (3.7). Thus, from (8.2),

$$\Theta'(\bar{\lambda}) = -2(\beta \sin \tfrac{1}{2}\theta)^{-1}. \tag{8.4}$$

The usual semiclassical singularity in forward scattering by potentials having long-range tails arises from the combined effect, as $\theta \to 0$, of the axial focusing singularity from the factor $(\sin\theta)^{-1/2}$ in (8.1) with the vanishing of $\Theta'(\bar{\lambda})$ as $\bar{\lambda} \to \infty$, corresponding to the small deflections at large impact parameters (Berry 1969).

In the present case, however, by (3.7), forward scattering is associated with $\bar{\lambda} \to \beta$, where $\Theta(\bar{\lambda})$ has a vertical tangent (figure 2). The corresponding singularity of (8.4) as $\theta \to 0$ cancels out the divergence arising from $(\sin\theta)^{-1/2}$ in (8.1), yielding the first term of (3.8), which is regular at $\theta = 0$.

Nevertheless, there is still a semiclassical singularity as $\theta \to 0$, but it is a subtler effect that appears in the first-order correction to (8.1), which contains terms proportional to (Nussenzveig 1965, equation (6.12)) $[\Theta''(\bar{\lambda})]^2/|\Theta'(\bar{\lambda})|^3$, $\Theta'''(\bar{\lambda})/[\Theta'(\bar{\lambda})]^2$. These terms give rise to the characteristic $(\beta \sin^3 \frac{1}{2}\theta)^{-1}$ singularity in (3.8).

The effective 'potential' for radial motion associated with λ is (figure 3)

$$U_{\text{eff}}(\lambda, r) = \begin{cases} \infty & r \leq a \\ \lambda^2/r^2 & r > a \end{cases} \tag{8.5}$$

which is the sum of the hard core with the centrifugal potential in the semiclassical approximation, i.e. including the Langer modification (Berry and Mount 1972).

The critical angular momentum $\lambda_c = \beta$ is associated with grazing incident rays. For $\lambda > \lambda_c$, as shown in figure 3, we find a turning point at

$$r_0 = \lambda/k \qquad \lambda > \lambda_c. \tag{8.6}$$

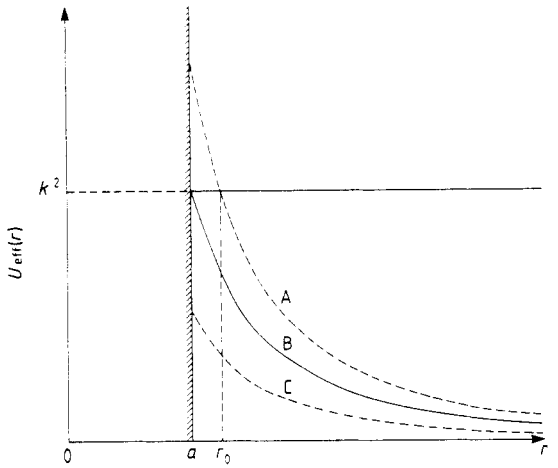

Figure 3. The effective 'potential' $U_{\text{eff}}(\lambda, r)$ (equation (8.5)) for $\lambda > \lambda_c$ (A), $\lambda = \lambda_c$ (B) and $\lambda < \lambda_c$ (C), where $\lambda_c = \beta$. r_0 = turning point for $\lambda > \lambda_c$.

The corresponding WKB barrier penetration factor up to the surface of the sphere is

$$v_\lambda = \exp\left(-2\int_{r_0}^{a} (\lambda^2/r^2 - k^2)^{1/2}\,\mathrm{d}r\right) \qquad \lambda > \beta. \tag{8.7}$$

It can readily be verified that (8.7) is identical to the exponential factor in (5.10), taking into account (5.3) and (5.4). Thus the above-edge integrand in (5.15) is weighted by the barrier penetration factor associated with tunnelling of the above-edge rays through the centrifugal barrier to the surface of the sphere. This is the origin of the rapid decay of the integrand.

While the uniform approximation is not expressed in terms of action functions along classical paths (Berry 1969), we see that the edge contribution is related to complex (tunnelling) paths that are complex extensions of classical paths, rather like instantons.

8.2. Physical interpretation of the edge contributions

Fock's own interpretation of his theory of diffraction by a curved edge (Fock 1965, chs 5 and 9) is in terms of transverse diffusion, a concept introduced by Leontovich (1944).

In geometrical optics, as is well known (Sommerfeld 1954), there are prescriptions for transport of the amplitude along rays, but no restrictions on its behaviour along transverse directions, so that discontinuities and other singularities are allowed. Leontovich and Fock interpret diffraction as a process of transverse diffusion of the amplitude along wave fronts.

This interpretation is based upon a local approximation to the reduced wave equation in a neighbourhood of the edge of a curved surface, in 'ray coordinates'. The relevant rays are the diffracted rays introduced by Keller in his geometrical theory of diffraction (Keller 1958). Figure 4 shows a tangentially incident ray AT and the corresponding diffracted ray TT'P leaving the surface tangentially at T' to reach the observation point P. The ray coordinates are the arc $\overset{\frown}{\mathrm{TT}'} = \eta$ described along the surface and the length

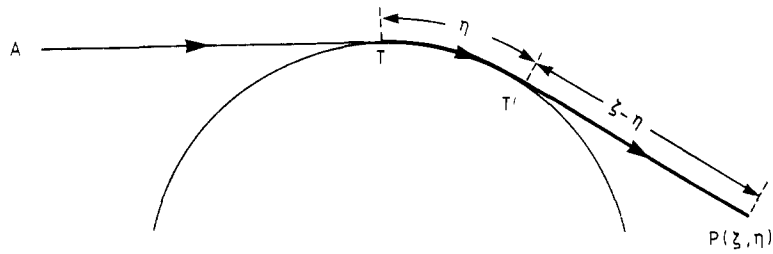

Figure 4. The ray coordinates (η, ζ) of an observation point P.

$\overset{\frown}{TT'} + \overline{T'P} = \zeta$ of the diffracted ray path. In the coordinates

$$x = b\zeta \qquad y = d(\zeta - \eta)^2 \tag{8.8}$$

where b and d are suitably defined constants, the reduced wave equation in a neighbourhood of T takes the form

$$i\partial\psi/\partial x = (-\partial^2/\partial y^2 - y)\psi(x, y). \tag{8.9}$$

According to the Leontovich-Fock interpretation, (8.9) describes transverse diffusion of the amplitude along wave fronts, leading to diffraction. Actually, in view of the imaginary coefficient, this interpretation is inadequate.

The proper analogy is with Schrödinger's equation, and (8.9) can be readily interpreted in our problem in terms of complex angular-momentum theory. Time evolution is replaced by evolution in x, i.e. along a ray, and y describes transverse behaviour, playing the role of a radial coordinate: $y = 0$ at the surface (which is a caustic of diffracted rays) and $y > 0$ above it. Thus (8.9) is analogous to the time-dependent radial Schrödinger equation for motion in a linear potential barrier, corresponding to motion near the top of the centrifugal barrier in figure 3, where it can be approximated by a linear potential.

The 'stationary' solutions are Airy functions, and we can build the 'time-dependent' solution as a wavepacket of stationary solutions. By requiring it to satisfy the boundary condition at the surface, as well as the excitation condition associated with the incident plane wave, we obtain the Fock-type functions. We may regard this as a higher-dimensional extension of the joining-up problem across a turning point in the one-dimensional WKB approximation (Berry and Mount 1972).

As was pointed out following (8.7), the function $H_+(x, \varphi)$ in (5.15) is essentially equivalent, for $x \gg 1$, to the centrifugal barrier penetration factor at the associated value of the impact parameter. Indeed, for arbitrary x, it corresponds to the uniform approximation (Berry and Mount 1972) to this penetration factor.

While the below-edge amplitude arises from the strong reflection effects near the barrier top, its complex angular momentum representation (6.14) can also be interpreted as a tunnelling amplitude. The rapid decay in (6.8) is the below-edge counterpart of (5.10): $H_-(x, \psi)$ and $H_+(x, \varphi)$ behave in a nearly symmetrical way for $x \gg 1$. Since ψ is the angle of incidence associated with the impact parameter $b = \lambda/k$ (cf (6.2)), we can also interpret $H_-(x, \psi)$ as a uniform barrier penetration factor for the complex angle of incidence ψ (see (6.13)). Thus the full edge amplitude (2.15) can be interpreted as a sum over complex paths, associated with tunnelling near the top of the centrifugal barrier (Nussenzveig and Winscombe 1987).

Diffraction, in the classical Huygens-Fresnel-Kirchhoff theory, is pictured as a disturbance of wave propagation due to the removal of a portion of the wavefronts by the blocking effect of the obstacle. This bulk blocking effect leads to the Airy diffraction pattern, which is uniformly represented here by (4.5). The classical diffraction amplitude is indeed dominant at very small diffraction angles, $\theta \leqslant \beta^{-1}$. However, classical diffraction theory completely fails to describe what happens at larger angles of diffraction, $\theta \geqslant \gamma$.

Large-angle diffraction around the curved edge of the sphere is described by the edge amplitude $F_e(\beta, \theta)$, which, as we have just seen, is a tunnelling amplitude. For $\theta \gg \gamma$, the remnants of tunnelling appear in the form of surface waves. Indeed (cf (2.25)), the surface-wave amplitude is generated by a combination of above-edge and below-edge terms. According to the geometrical theory of diffraction (Keller 1958), 'creeping waves' are generated by tangentially incident rays. We now see that, in a more complete wave picture, they are actually launched by tunnelling which takes place within the entire edge domain.

This interpretation of diffraction as tunnelling into 'classically forbidden' regions extends to more general curved surfaces, with the centrifugal barrier replaced by more general inertial barriers in suitable curvilinear coordinates (Beck and Nussenzveig 1960).

9. Discussion

According to § 3, the outer approximation is expected to become accurate only for $\theta \gg \gamma$, where (cf § 7) the Fock approximation can no longer be applied. Thus, the domains of validity of these two approximations do not overlap: they cannot be joined to yield accurate results for all θ.

The uniform approximation must also break down at large enough θ, since the asymptotic expansions on which it is based lose their validity as $\theta \to \pi$. However, its domain of applicability certainly extends to $\theta \gg \gamma$, allowing us to join it up with the outer approximation. This leads to accurate expressions for $F(\beta, \theta)$ over the whole range $0 \leqslant \theta \leqslant \pi$.

The residue series appearing in these expressions are rapidly convergent: only their first few terms need to be retained. The integrands of (5.15), (6.14), (6.25) and (6.29) are all smooth and of faster than exponential decrease, so that one can cut them off as indicated in (6.33) (for (6.25), in view of the exponential decay of $\mathscr{P}^{(2)}$, an even lower cutoff, $c = 3$, may be taken).

There remains the definite integral (6.27), which behaves like a Fresnel integral near its upper limit t. One can estimate from (6.16) and (6.21) that the integrand of (6.27) goes through $\sim\frac{2}{3}(\theta/2\gamma)^3$ cycles of oscillation within the range of integration. This number increases rapidly for $\theta \gg \gamma$. Thus, although contributions from beyond the range of the stationary phase point $\bar{t}$ tend to cancel out by destructive interference, it is convenient to shift over to the outer approximation as soon as this can be done without loss of accuracy. The WKB approximation should be rejoined by the time the integrand has gone through one or two cycles of oscillation, which (for large enough β) occurs around $\theta \sim 4.5\gamma$.

In figure 5, the uniform, outer and Fock approximations to $|F(\beta, \theta)|$ and arg $F(\beta, \theta)$ for $\beta = 10$ are compared with the exact partial-wave solution (in view of the rapid variation of arg F, we have plotted $\cos(\arg F + 2\beta \sin\frac{1}{2}\theta + \pi)$, which, by (3.8), is better

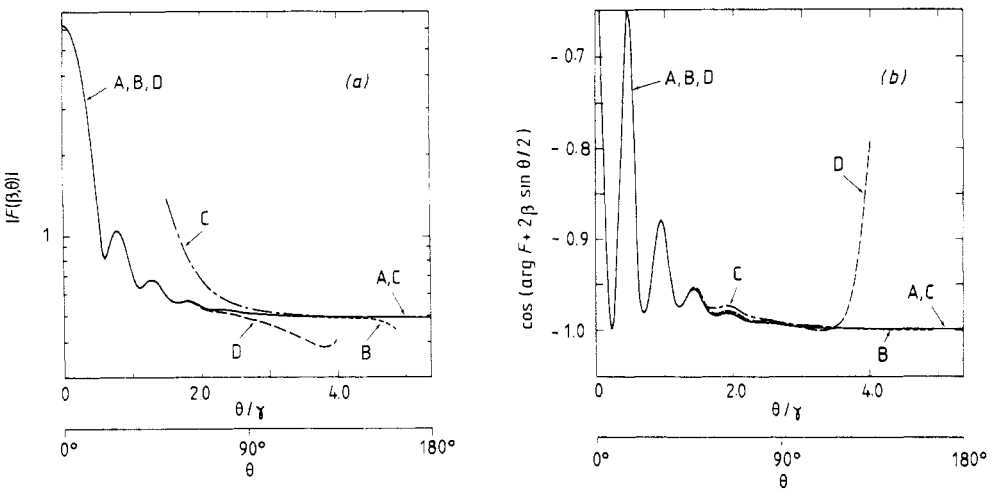

Figure 5. (*a*) $|F(\beta, \theta)|$ for $\beta = 10$: exact (A) compared with uniform (B), outer (C) and Fock (D) approximations. (*b*) Same for $\cos(\arg F + 2\beta \sin \frac{1}{2}\theta + \pi)$.

behaved). The magnitudes of the relative errors associated with the various approximations are plotted in figure 6. The numerical evaluation of the partial-wave solution was performed by applying techniques similar to those developed by Wiscombe (1980).

The relative error of the uniform approximation to $|F|$ starts out at $\leqslant 3$ parts per million at $\theta = 0°$ and it stays below 0.01% for $\theta < 70°$. At the crossover with the relative error curve for the outer approximation, which here occurs at $\theta \sim 3.7\gamma$, we find the maximum error of the combined approximation, about 0.3%. The relative errors for the Fock approximation are one to two orders of magnitude larger than those for the uniform approximation up to $\theta \sim 1.5\gamma$, and they grow very rapidly beyond this range. The results for the phase of F are similar.

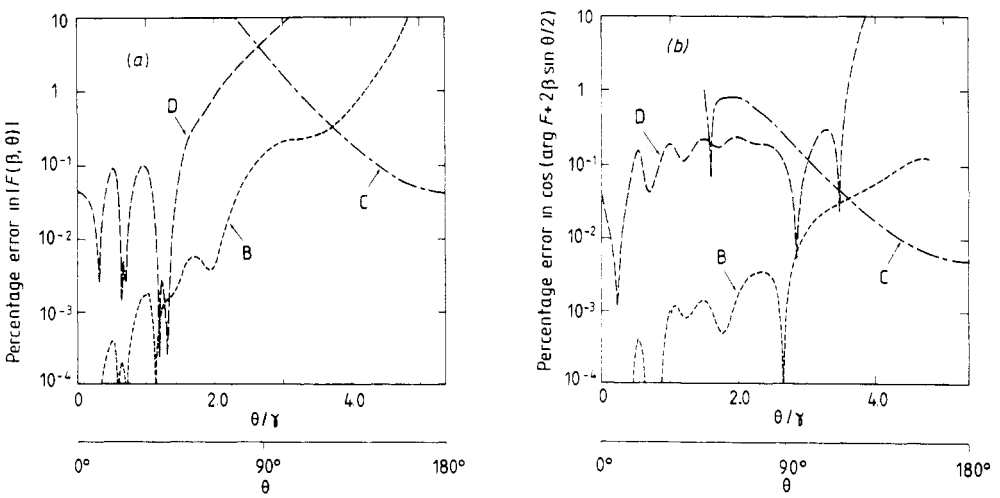

Figure 6. (*a*) Magnitudes of the relative errors of the approximations plotted in figure 5(*a*); (*b*) same for figure 5(*b*).

The small oscillations of $|F|$ in the outer approximation result from the interference between the contributions of reflected waves (WKB) and surface waves. We see in figure 5 that they are just the continuation of the oscillations found in the uniform approximation, which arise mainly from the edge amplitude. This agrees with our interpretation of large-angle diffraction in terms of tunnelling (§ 8).

We have not plotted what might be called the 'classical' approximation,

$$F_{\mathrm{cl}}(\beta, \theta) = \mathrm{i}\, J_1(\beta\theta)/\theta - \tfrac{1}{2}\exp(-2\mathrm{i}\beta \sin \tfrac{1}{2}\theta) \tag{9.1}$$

the sum of the classical diffraction amplitude (van de Hulst 1957) and the WKB reflection amplitude. This would be a very poor approximation, yielding a displaced diffraction pattern, with much stronger contrast between maxima and minima. Naturally, the classical diffraction amplitude is not expected to be applicable at large θ.

The magnitudes of the relative errors of the uniform and Fock approximations to the extinction efficiency, given by (6.34) and (7.15), respectively, are plotted in figure 7 for $\frac{1}{2} \leqslant \beta \leqslant 10$. The relative error of the uniform approximation is ~ 1.3 parts per million at $\beta = 10$, rising monotonically as β decreases, but still remaining below 1% at $\beta = \frac{1}{2}$. For the Fock approximation, even though $O(\beta^{-2})$ corrections are included in (7.15), the relative error remains about one order of magnitude larger.

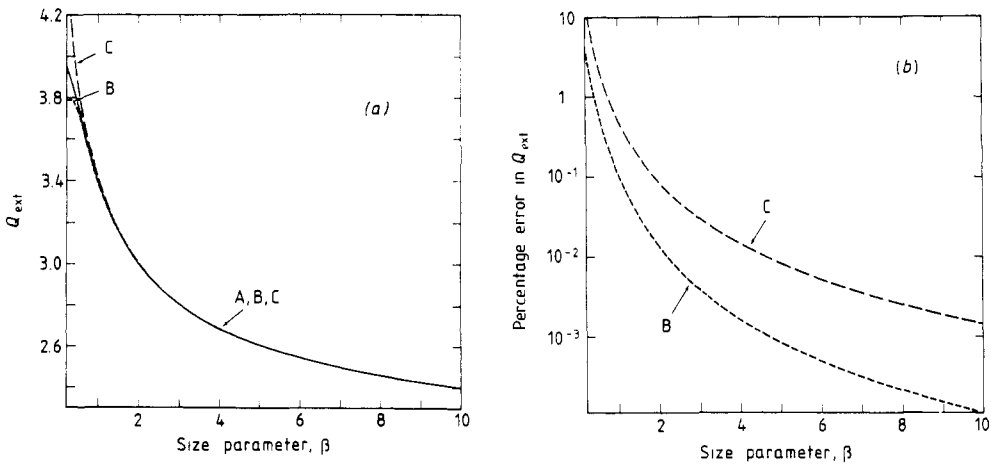

Figure 7. (*a*) Extinction efficiency $Q_{\mathrm{ext}}(\beta)$, for $\frac{1}{2} \leqslant \beta \leqslant 10$: exact (A) compared with uniform (B) and Fock (C). (*b*) Magnitudes of the relative errors of the approximations plotted in (*a*).

More detailed numerical comparisons (Nussenzveig and Wiscombe 1987) confirm that the combined uniform and outer approximation remains accurate all the way down to $\beta \sim 1$, bridging the gap between short- and long-wavelength scattering. The accuracy is, typically, one to two orders of magnitude better than that of the Fock approximation within its range of applicability. The maximum error decreases from a few per cent for $\beta \sim 1$ to $\leqslant 0.3\%$ for $\beta \geqslant 10$ and $\leqslant 0.02\%$ for $\beta \geqslant 100$.

The maximum error is not a good measure of the accuracy because it tends to occur in the backward hemisphere where the differential cross section is small. In the region that yields most of the contribution to the cross section, typical errors are one to two orders of magnitude below the maximum error. The phase accuracy is even

better than that for $|F|$. For large values of β, the relative error of the uniform approximation becomes so small that it is hard to estimate, since this would require pushing the accuracy of partial-wave summations beyond its usual limits. For practical purposes, the uniform approximation becomes indistinguishable from the exact solution.

We conclude that complex angular-momentum theory provides a rather thorough understanding of the scattering by an impenetrable sphere. In particular, large-angle diffraction can be interpreted as a tunnelling effect.

Acknowledgments

It is a pleasure to thank Dr W J Wiscombe for helpful discussions and for the plots in figures 5-7. This work was done while the author held a National Research Council-NASA Research Associateship.

Appendix 1. Asymptotic expansions of special functions

Olver's uniform asymptotic expansions of Hankel's functions $H_\lambda^{(1,2)}(\beta)$ for large $|\lambda|$ are (Olver 1974)

$$H_\lambda^{(1,2)}(\beta) = 2\exp(\mp i\pi/3)\left(\frac{4\xi}{1-z^2}\right)^{1/4}\left(\frac{\mathrm{Ai}(\exp(\pm 2i\pi/3)\lambda^{1/3}\xi)}{\lambda^{1/3}}\sum_{k\geqslant 0}\frac{a_k(\xi)}{\lambda^{2k}}\right.$$
$$\left.+\exp(\pm 2i\pi/3)\frac{\mathrm{Ai}'(\exp(\pm 2i\pi/3)\lambda^{1/3}\xi)}{\lambda^{5/3}}\sum_{k\geqslant 0}\frac{b_k(\xi)}{\lambda^{2k}}\right) \tag{A1.1}$$

where Ai denotes the Airy function, and, depending on the relative magnitudes of λ and β, one may choose either one of the representations

$$z^{-1} = \lambda/\beta = \cosh\varphi \qquad \tfrac{2}{3}\xi^{3/2} = \varphi - \tanh\varphi \tag{A1.2}$$

$$z^{-1} = \lambda/\beta = \cos\psi \qquad \tfrac{2}{3}(-\xi)^{3/2} = \tan\psi - \psi \tag{A1.3}$$

the branches being such that ξ is real for real λ and $z>0$. The coefficients a_k and b_k are given by Olver (1974). In particular,

$$a_0(\xi) = 1 \tag{A1.4}$$

$$b_0(\xi) = -\frac{5}{48\xi^2} + \frac{1}{\xi^{1/2}}\left(\frac{5}{24(1-z^2)^{3/2}} - \frac{1}{8(1-z^2)^{1/2}}\right)$$
$$= -\frac{5}{48\xi^2} + \frac{1}{(-\xi)^{1/2}}\left(\frac{5}{24(z^2-1)^{3/2}} + \frac{1}{8(z^2-1)^{1/2}}\right). \tag{A1.5}$$

We have (Abramowitz and Stegun 1964, p 446)

$$\mathrm{Ai}(\exp(\pm 2i\pi/3)x) = \tfrac{1}{2}\exp(\pm i\pi/3)[\mathrm{Ai}(x) \mp i\,\mathrm{Bi}(x)] \tag{A1.6}$$

with the Wronskian

$$W[\mathrm{Ai}(x), \mathrm{Bi}(x)] = 1/\pi. \tag{A1.7}$$

The uniform asymptotic expansion of $J_\lambda(\beta) = \frac{1}{2}[H_\lambda^{(1)}(\beta) + H_\lambda^{(2)}(\beta)]$ follows from (A1.1) and (A1.6).

For $|\lambda^{1/3}\xi| \gg 1$ in (A1.1), we can employ the asymptotic expansions of $\mathrm{Ai}(z)$ and $\mathrm{Ai}'(z)$ (Abramowitz and Stegun 1964, p 448):

$$\mathrm{Ai}(z) \approx \frac{\exp(-\frac{2}{3}z^{3/2})}{2\sqrt{\pi}z^{1/4}}\left(1-\frac{5}{48z^{3/2}}+\mathrm{O}(z^{-3})\right) \qquad |z| \gg 1 \qquad |\arg z| < \pi \tag{A1.8}$$

$$\mathrm{Ai}'(z) \approx -\frac{z^{1/4}}{2\sqrt{\pi}}\exp(-\tfrac{2}{3}z^{3/2})\left(1-\frac{7}{48z^{3/2}}+\mathrm{O}(z^{-3})\right) \qquad |z| \gg 1 \qquad |\arg z| < \pi \tag{A1.9}$$

and (A1.1) reduces to Debye's asymptotic expansion (Abramowitz and Stegun 1964, p 366)

$$H_\lambda^{(1,2)}(\beta) = \left(\frac{2}{\pi\beta\sin\psi}\right)^{1/2}\exp\{\pm\mathrm{i}[\beta(\sin\psi-\psi\cos\psi)-\tfrac{1}{4}\pi]\}$$
$$\times\left(1\mp\frac{\mathrm{i}}{8\beta\sin\psi}(1+\tfrac{5}{3}\cot^2\psi)+\mathrm{O}(\lambda^{-2})\right) \tag{A1.10}$$

for (A1.3), with a corresponding result for (A1.2).

The Szegö-Olver uniform asymptotic expansion of $P_{\lambda-1/2}(\cos\theta)$ for large $|\lambda|$ is given by (Olver 1974)

$$P_{\lambda-1/2}(\cos\theta) \approx \mathscr{P}(\theta,\lambda) \tag{A1.11}$$

where

$$\mathscr{P}(\theta,\lambda) \equiv \left(\frac{\theta}{\sin\theta}\right)^{1/2}\left\{\left[1+\frac{1}{128\lambda^2}\left(1-\frac{9}{\sin^2\theta}-6\frac{\cot\theta}{\theta}+\frac{15}{\theta^2}\right)\right]J_0(\lambda\theta)\right.$$
$$\left.-\frac{1}{8\lambda}\left(\frac{1}{\theta}-\cot\theta\right)J_1(\lambda\theta)+\mathrm{O}(\lambda^{-3})\right\}. \tag{A1.12}$$

The corresponding uniform asymptotic expansions for $Q_{\lambda-1/2}^{(1,2)}(\cos\theta)$ (cf (2.9)) are

$$Q_{\lambda-1/2}^{(1,2)}(\cos\theta) \approx \mathscr{P}^{(1,2)}(\theta,\lambda) \tag{A1.13}$$

where

$$\mathscr{P}^{(1,2)}(\theta,\lambda) \equiv \left(\frac{\theta}{\sin\theta}\right)^{1/2}\left\{\frac{1}{2}\left[1+\frac{1}{128\lambda^2}\left(1-\frac{9}{\sin^2\theta}-6\frac{\cot\theta}{\theta}+\frac{15}{\theta^2}\right)\right]H_0^{(2,1)}(\lambda\theta)\right.$$
$$\left.-\frac{1}{16\lambda}\left(\frac{1}{\theta}-\cot\theta\right)H_1^{(2,1)}(\lambda\theta)+\mathrm{O}(\lambda^{-3})\right\}. \tag{A1.14}$$

Note that $\mathscr{P}^{(1)}$ is associated with $H_0^{(2)}$ and $\mathscr{P}^{(2)}$ with $H_0^{(1)}$.

For $|\lambda|\theta \gg 1$, (A1.13) goes over into (Robin 1958)

$$Q_{\lambda-1/2}^{(1,2)}(\cos\theta) = \frac{\exp[\mp\mathrm{i}(\lambda\theta-\frac{1}{4}\pi)]}{(2\pi\lambda\sin\theta)^{1/2}}\left[1\pm\frac{\mathrm{i}\cot\theta}{8\lambda}+\frac{1}{128\lambda^2}\right.$$
$$\left.\times\left(1-\frac{9}{\sin^2\theta}\right)+\mathrm{O}(\lambda^{-3})\right] \qquad |\lambda|\theta \gg 1. \tag{A1.15}$$

Appendix 2. Inversion of (5.4) and (6.3)

Employing the power series expansions of $\cosh\varphi$ and $\sinh\varphi$, (5.4) may be rewritten as

$$\varphi\cosh\varphi-\sinh\varphi = 2\varphi^3/3!+4\varphi^5/5!+6\varphi^7/7!+\ldots = \tfrac{1}{3}\varphi_0^3(x) \tag{A2.1}$$

where

$$\varphi_0(x) \equiv \gamma\sqrt{x}. \tag{A2.2}$$

To lowest order, (A2.1) yields $\varphi(x) \approx \varphi_0(x)$, suggesting a solution of the form

$$\varphi(x) = \varphi_0(1 + c_1\varphi_0^2 + c_2\varphi_0^4 + \ldots). \tag{A2.3}$$

Substituting (A2.3) into (A2.1) and identifying the coefficients of similar powers of φ_0, one determines the unknown expansion coefficients $c_1, c_2, \ldots$, leading to (5.13).

Similarly, (6.3) may be rewritten as

$$\sin\psi - \psi\cos\psi = 2\psi^3/3! - 4\psi^5/5! + 6\psi^7/7! - \ldots = \tfrac{1}{3}\psi_0^3(x) \tag{A2.4}$$

where

$$\psi_0(x) \equiv \exp(-i\pi/6)\gamma\sqrt{x}. \tag{A2.5}$$

We look for the solution in the form

$$\psi(x) = \psi_0(1 + d_1\psi_0^2 + d_2\psi_0^4 + \ldots). \tag{A2.6}$$

Substituting into (A2.4) and identifying, we find $d_1, d_2, \ldots$, leading to (6.11).

Appendix 3. Reduction to generalised Fock functions

It follows from (7.9) and Nussenzveig (1969, equation (C.3)) that

$$\mathscr{F}_{0,0}(\beta,\theta) + \tfrac{1}{2}\gamma^2\mathscr{F}_{1,0}(\beta,\theta) = -(\gamma/\theta)J_1(\beta\theta) + (\gamma/\theta)[F_{0,1}(\beta,\theta) + \tfrac{1}{2}\gamma^2 F_{1,1}(\beta,\theta)]. \tag{A3.1}$$

On the other hand, we have

$$J_1(\beta\theta + \theta x/\gamma) = -\frac{\gamma}{\theta}\frac{d}{dx}J_0(\beta\theta + \theta x/\gamma).$$

Substituting this into (7.9), with $m = 2$, $n = 1$, and integrating by parts, we obtain (cf (7.10))

$$\mathscr{F}_{2,1}(\beta,\theta) = 2(\gamma/\theta)\mathscr{F}_{1,0}(\beta,\theta) - (\gamma/\theta)F_{2,0}(\beta,\theta) \tag{A3.2}$$

where we have also employed the relationship

$$\frac{d}{dx}\left(\frac{\mathrm{Ai}(x)}{\mathrm{Ai}(\exp(\pm 2i\pi/3)x)}\right) = -\frac{\exp(\mp i\pi/6)}{2\pi\,\mathrm{Ai}^2(\exp(\pm 2i\pi/3)x)} \tag{A3.3}$$

which follows from the Wronskian relation (5.9).

Substituting (A3.1) and (A3.2) into (7.8), we get (7.11).

References

Abramowitz M and Stegun I A 1964 *Handbook of Mathematical Functions* (Washington, DC: National Bureau of Standards)

Beck G and Nussenzveig H M 1960 *Nuovo Cimento* **16** 416

Berry M V 1969 *J. Phys. B: At. Mol. Phys.* **2** 381

Berry M V and Mount K E 1972 *Rep. Prog. Phys.* **35** 315

Bleistein N and Handelsman R A 1975 *Asymptotic Expansions of Integrals* (New York: Holt, Rinehart and Winston)
Borovikov V A and Kinber B Ye 1974 *Proc. IEEE* **62** 1416
Fock V A 1965 *Electromagnetic Diffraction and Propagation Problems* (Oxford: Pergamon)
Keller J B 1958 *Calculus of Variations and its Applications* ed L M Graves (New York: McGraw-Hill) p 27
Keller J B, Lewis R M and Seckler B D 1956 *Commun. Pure Appl. Math.* **9** 207
Leontovich M A 1944 *Bull. Acad. Sci. USSR* **8** 16
Lewis R M, Bleistein N and Ludwig D 1967 *Commun. Pure Appl. Math.* **20** 295
Lisle I G, Parlange J Y, Rand R H, Hogarth W L, Braddock R D and Gottlieb H P 1985 *Phys. Rev. Lett.* **55** 555
Logan N A 1959 *General Research in Diffraction Theory* vols 1 and 2 (Sunnyvale: Lockheed Missiles and Space Division)
Logan N A and Yee K S 1962 *Electromagnetic Waves* ed R E Langer (Madison, WI: University of Wisconsin Press) p 139
Ludwig D 1966 *Commun. Pure Appl. Math.* **19** 215
—— 1967 *Commun. Pure Appl. Math.* **20** 103
—— 1969 *Commun. Pure Appl. Math.* **22** 715
Malyuzhinets G D 1959 *Sov. Phys.-Usp.* **69** 749
Nussenzveig H M 1965 *Ann. Phys., NY* **34** 23
—— 1969 *J. Math. Phys.* **10** 82
—— 1979 *J. Opt. Soc. Am.* **69** 1068
Nussenzveig H M and Wiscombe W J 1987 *Phys. Rev. Lett.* to be published
Olver F W J 1974 *Asymptotics and Special Functions* (New York: Academic)
Robin L 1958 *Fonctions Sphériques de Legendre et Fonctions Sphéroïdales* vol II (Paris: Gauthier-Villars)
Sengupta D L 1969 *Electromagnetic and Acoustic Scattering by Simple Shapes* ed J J Bowman, T B A Senior and P L E Uslenghi (Amsterdam: North-Holland) ch 10
Senior T B A 1965 *University of Michigan Radiation Laboratory Report* no 70310-1-T
Sommerfeld A 1954 *Optics* (New York: Academic) § 35
Streifer W and Kodis R D 1964 *Q. Appl. Math.* **21** 285
van de Hulst H C 1957 *Light Scattering by Small Particles* (New York: Wiley)
Wiscombe W J 1980 *Appl. Opt.* **19** 1505
Wu T T 1956 *Phys. Rev.* **104** 1201